Disc surface modifications for enhanced performance against friction noise

D.W. Wang [a], J.L. Mo [a, *], X.H. Ge [a], H. Ouyang [b], Z.R. Zhou [a]

[a] *Tribology Research Institute, Southwest Jiaotong University, Chengdu 610031, China*

[b] *School of Engineering, University of Liverpool, Liverpool L69 3GH, UK*

Abstract:

Surface modifications of metal discs in the form of parallel and radial grooves are investigated for acquiring enhanced performance against friction-induced noise. Experimental and numerical studies indicate that grooved surfaces are capable of reducing squeal noise, and the groove width significantly affects the squeal noise level. Moreover, a disc sample with parallel grooves distributed on only half of surface well verifies the ability of grooves in reducing squeal noise generation. Numerical analysis is further performed to give an explanation on how the grooves can reduce squeal noise and why the disc samples with different groove widths exhibit different performance in reducing squeal noise.

Key words: Surface modification; texture; grooves; friction; friction noise.

1. Introduction

Brake noise can easily occur during the last stage of a braking action, which is usually undesirable and often associated with various friction problems such as excessive wear and surface damage of the brake components. Therefore, it has become one of the most important rating items in the vehicle initial quality standard test. Brake noise in different frequency ranges has been described by a number of terminologies, such as grunt, chatter, judder, moan, groan, squeak and squeal, etc. [1]. Among them, brake squeal having high frequency (usually above 1 kHz) and high sound pressure levels (usually above 78 dB) has been regarded as the most troublesome and annoying type of noise, because of its detrimental effect on the comfort of passengers and the brand image of vehicles [2-4]. Therefore, seeking an effective method to reduce and eliminate brake squeal is required, and has become a challenging subject for automotive engineers and researchers.

*Corresponding author. Tel.: +86-28-87600601; fax: +86-28-87603142.

E-mail address: jlmo@swjtu.cn (J.L. Mo)

Over the past few decades, a large amount of effort has been made on identifying the main source of squeal generation. Mills [5] found that the negative friction coefficient with respect to the relative sliding speed played a key role in the friction instability. Spurr [6] indicated that self-excited vibration of a friction system depended on the contact area and friction coefficient. North [7] attributed friction-induced vibration to the coalescence of two adjacent eigenfrequencies of the system, and this theory was termed as 'mode coupling'. In addition, Ouyang et al. [8] provided a detailed account of moving loads concept and illustrated that the brake squeal propensity was related to the rotational speed of brake disc. Graf and Ostermeyer [9] recently applied a new dynamic friction law to a simple model and found that squeal instability would occur in region with positive friction-velocity slopes. It is no doubt that those findings are significant for better understanding of friction noise. However, the underlying mechanisms of friction noise generation are still not fully understood and none of the above-mentioned theories can well explain all the phenomena related to friction noise, thus a thorough solution for elimination of squeal noise still seems to be an elusive goal [10].

In the case of brake squeal produced during braking, the surface topography is found to play a significant role in affecting the contact stiffness and wear performance of contact interface, which would consequently determine the dynamic instability and squeal generation of the friction system [11-17]. Researchers from Uppsala University conducted extensive research on identifying the relationship between microscopic surface topography of brake components and the occurrence of brake squeal [11-14]. In addition, AbuBakar et al. [15] introduced the real pad topography to a finite element model of a real disc brake system and verified that the squeal instability of brake system could vanish at particular surface topography. Shin et al. [16] found that the size of the zircon particles in the friction material would affect the contact stiffness of interface and consequently the characteristics of friction instability. Hetzler et al. [17] introduced tribological contact parameters into a brake model and found that the microscopic contact properties had a significant effect on the stability of the system. Yoon et al. [18] observed that the size of the surface contact plateaus significantly affected the propensity of dynamic instability and wear performance. Lee et al [19] indicated that the surface roughness strongly affected the normal contact stiffness of interface, and accordingly determined the friction oscillation pattern. Lazim et al. [20] conducted brake squeal tests and found that the damage of pad surface was relevant to the squeal event. Magnier et al. [21] studied the influence of contact states on friction-induced vibration and found that the stiffness heterogeneities of the contact surface could significantly affect the lock-in modes. Duffour and Woodhouse [22] investigated the effect of uncertainty contact

parameters on the squeal instability, and quantified the capability of this uncertainty on squeal predictions. Butlin and Woodhouse [23] performed a systematic experimental study of squeal initiation and explored the sensitivity of predictions to parameter variations.

These studies indicate that there is a strong relationship between microscopic surface topography and the generation of squeal noise. However, the microscopic topography possesses random characteristics, which results in the uncontrollability of contact states and relatively poor repeatability of experimental results. Therefore, more and more researchers try to create customised surfaces with good regularity to investigate their effect on the generation of squeal, and seek for an effective way to reduce squeal noise [24-26].

Nowadays, textured surfaces with their good geometric repeatability have been widely used in the field of tribology [27-30]. However, most of relevant studies focused on investigating the ability of textured surfaces in improving the friction and wear properties, and the effect of textured surface on squeal characteristics is rarely reported, and the knowledge about the influence of textured surface on squeal noise properties is very limited [26, 31]. Therefore, studying the relation between the textured surface and squeal generation is extremely worthwhile, which may help provide a further understanding of the generation of squeal and also for optimal design of customised surfaces to reduce squeal noise of brake system.

In this work, two kinds of surface modifications of discs in the form of: grooves at parallel regular intervals (i.e. parallel grooves), and grooves at radial regular angular intervals (i.e. radial grooves) were manufactured on the disc surfaces, respectively. Experimental tests of friction noise were performed in a pad-on-disc configuration to study the capability of grooved surface in reducing squeal noise. Moreover, a numerical study was performed to provide a possible physical explanation for the experimental phenomenon.

2. Experimental details

2.1 Description of experimental setup

For investigating brake squeal, a pad-on-disc setup is used. This simplified physical system is less complex than a real brake system but possesses the essential features of a real brake system, which permits the occurrence of modes lock-in between the components through a friction interface at a reduced scale. The image of the experimental setup is given in Fig. 1. The disc sample is driven at a certain speed by the rotary motor, and the pad sample is fixed in the upper pad holder, which is pressed down to rubbing against the lower disc sample and attached with a 2-D strain-gauge force sensor (CETR DFH-50: measurement range of 5

N~500 N and resolution of 0.025 N). A real-time recording of the vibration signals is performed by using a 3-D acceleration sensor (KISTLER 8688A50: measurement ranges of ±50 g, frequency ranges of 0.5 Hz~5 kHz and sensitivity of 100 mV/g and mass of 6.5 g), which is mounted on the pad holder. A microphone (MTG MK250: dynamic range of 15 dB~146 dB, frequency range of 3.5 kHz~20 kHz and sensitivity of 50 mV/Pa) is placed nearby the contact surface to detect the sound signal. All the signals measured from sensors are recorded and analyzed synchronously by using a Müller-BBM 32-channels MKII equipment.

2.2 Preparation of samples

In this study, all the disc samples are cut from a compacted graphite iron brake disc of train to a diameter of 25 mm and thickness of 3 mm. The pad samples with length of 15 mm and cross section of 10 mm×10 mm are used as the counterface, which are cut from a composite material brake pad of train.

Two kinds of groove-textured surface configurations manufactured by milling are introduced: surface with grooves at parallel regular intervals (i.e. parallel grooves), and surface with grooves at radial regular angle intervals (i.e. radial grooves), as illustrated in Fig. 2. Moreover, a customised sample with parallel grooves distributed on only half of the disc surface is manufactured, to detect the evolution of vibration and noise from smooth surface to groove textured surface in one disc sample, and further validate the effect of grooves on the squeal generation. Abbreviations are defined as following: S represents disc sample with smooth surface, T-*w*-*x*-*y* represents groove-textured surface with pitch of *x* mm (for parallel grooves) or angle of *x*° (for radial grooves) and groove width of *y* mm distributed on the whole disc surface, T-*h*-*x*-*y* represents disc sample having groove-textured surface with pitch of *x* mm and groove width of *y* mm distributed on only half of the disc surface.

In the tribological tests, a normal load of 100 N and a disc rotating speed of 60 rpm are used, and a testing duration of 1800 s is set. The middle of pad contact surface is at a distance of 6 mm from the centre of the disc. All the tests are conducted in strictly controlled dry atmospheric working conditions (room temperature of 24~27℃, relative humidity of 60±10% RH). All the disc samples are ultrasonic cleaned with acetone prior to the test. The test for each kind of surface is repeated at least three times, in order to obtain the test results with good repeatability. After the tribological tests, the worn surfaces of the disc samples are examined by using optical microscopy.

3. Comparison of the smooth and grooved surfaces

3.1. Vibration and noise analysis

The average equivalent sound pressure levels generated from the smooth and grooved surfaces during the whole testing time are evaluated, as shown in Fig. 3. The background sound pressure level evaluated during the test is about 65 dB. It is found that the sound pressure of the smooth surface stays at a high level of about 100 dB throughout the whole test, while the sound pressure of all the grooved surfaces are significantly lower, which indicates that the metal discs with surface modifications have good potential in reducing squeal noise level compared with the smooth surface. Moreover, the sound pressure of discs having parallel grooves are found to decrease with increasing groove width and pitch, and the T-w-4-2 surface shows the most potential in squeal suppression among the three parallel grooved surfaces (Fig. 3(a)). For the discs having radial grooves, the sound pressure level is also found to decrease with the groove width increasing from 0.25 mm to 1 mm (Fig. 3(b)).

Furthermore, the effect of grooves on the distribution of frequency and its energy density is studied by performing time-frequency analysis for the noise signals of the smooth and grooved surfaces, as shown in Fig. 4. The noise generated from all the smooth and grooved surfaces is found to share one fundamental frequency of 1175 Hz accompanied with its high-order harmonics. However, the grooved surfaces show much better performance in reducing energy density in the excited frequencies, particularly for the T-w-4-2 surface showing significantly lower energy density in high frequencies. Therefore, surface modification of discs by using grooves is found to have little effect on the fundamental frequencies distribution of squeal noise, instead it can significantly change the energy densities contained in the excited frequencies and suppress the generation of some high-frequency squeal noise.

The time histories accelerations in both normal and friction directions and sound pressure signals are correspondingly studied, as shown in Fig. 5. The signals in the testing cycle of 1700-1701 s are analysed, as the squeal generation is steady in this stage. For the smooth surface, the vibration acceleration signals in both tangential and normal directions exhibit visible continuous high-frequency fluctuations, and accordingly squeal emissions throughout this cycle. In contrast, relatively minor and discontinuous high-frequency fluctuations of vibration accelerations are found for all the modified surfaces. The evolutions of vibration acceleration signals in both tangential and normal directions show a good correlation with those of the noise signal, suggesting that the friction noise is caused by the friction-induced vibration of the contact surfaces. The amplitudes of vibration accelerations

recorded from the grooved surfaces show smaller values and thus lower squeal noise compared with the smooth surface.

3.2 Friction analysis

The disc surface modification would change the contact states and consequently tribological properties during friction process. In Fig. 6, the friction force signals during the cycle of 1700-1701 s are illustrated to reveal how the grooves on the friction interface change the friction behaviour. The smooth surface exhibits significantly different friction force curve compared with the grooved surfaces. A number of visible wave-fluctuations can be observed for all friction force curves of the grooved surfaces. Moreover, the grooved surfaces show relatively lower value of friction force. This may be attributed to the variation of interface contact conditions when the pad sliding across the grooves. The existence of grooves may result in the variation of contact area and consequently the change of local contact stiffness, which may further affect the vibration instability and the generation of squeal noise.

4. The T-h-4-2 surface with parallel grooves distributed on only half of disc surface

4.1 Vibration and noise analysis

In order to further reveal the effect of grooved surface on the squeal noise as well as tribological properties, a customised disc sample with parallel grooves distributed on only half of surface is prepared. The size parameter of groove of pitch of 4 mm and width of 2 mm is selected considering that the grooved surface in this size exhibits the best performance in reducing squeal generation among the three parallel grooved surfaces. As a consequence, the effect of grooves on the squeal generation can be well validated by detecting the evolution of vibration accelerations, noise and friction force signals from smooth surface to grooved surface in just one disc surface. All the tribological testing parameters and conditions for this kind of sample are the same as above mentioned.

Fig. 7 shows the vibration acceleration and noise signals of the T-h-4-2 surface during the rotation cycle of 1700-1701 s. During the first half cycle during which the pad is sliding on grooved disc surface, no substantial increase in the amplitude of the vibration accelerations can be observed , and accordingly low sound pressure level is measured. In contrast, when the pad is mainly sliding on smooth disc surface in the second half cycle, continuous high-frequency fluctuations of the vibration accelerations in both normal and tangential directions are visible, which results in the significant squeal generation in this interval, as shown in Fig. 7(a-c). In addition, the equivalent sound pressure level as a function of time in this cycle is evaluated, as shown in Fig. 7(d). A visible shift in sound pressure level is

observed when the pad contact surface shifts from grooved surface to smooth surface, which is consistent with the interface vibration behaviour. Thus, quite different vibration and noise characteristics are observed in one cycle, and the change in squeal generation behaviour in the two half cycles can be attributed to their difference in surface morphologies.

The time-frequency analysis is further performed for the tangential vibration acceleration and sound pressure signals of the T-h-4-2 surface. In Fig. 8, it is found that a dominant frequency of 1175 Hz with high energy density occurs when the contact state gradually shifts from the pad-on-grooved surface to the pad-on-smooth surface, which highlights the capability of grooved surface in reducing squeal noise. Therefore, the existence of grooves on the disc surface is well validated to be able to reduce the energy density contained in the excited frequencies and consequently the squeal noise of the friction system.

4.2 Tribological analysis

Observation of the friction force curve shown in Fig. 9 indicates that grooves in the friction interface change the friction behaviour during the friction process, by the comparison of the different trends of friction force curve between the contact situations of pad-on-grooved surface and pad-on-smooth surface. Occurrence of visible wave-fluctuations in the friction force curve can be observed in the first half cycle of pad-on-grooved surface contact, which is different from the situation in the second half cycle of pad-on-smooth surface contact. A further explanation on how the groove changes the contact states and the friction behaviour will be performed in the following section 4.3.

Moreover, the worn surface morphology of the T-h-4-2 surface is observed by optical microscope after the test, as shown in Fig. 10. The region of smooth surface is found to undergo severe wear, with visible ploughing and detachment being observed in the wear track. In contrast, the ridge region between grooves shows different wear situations. No severe wear damage can be found on the ridge region, and there is a plenty of black wear debris existing inside the grooves. The grooves play a storage cavity role in trapping wear debris, and change the interface wear status. The wear of the grooved surface is mainly characterized by slight ploughing along the sliding direction.

4.3 Numerical analysis

4.3.1 Effect of grooves on contact pressure distribution

The experimental results show that the disc surface modification by using grooves is able to reduce the squeal noise generation. In this section, a numerical study is performed by using ABAQUS 6.10 to provide a possible physical explanation on why the disc with grooved

surface can reduce the tendency of squeal generation. A simplified finite element model of the experimental system is created and the constraint condition of the model is shown in Fig. 11. Five parts are included in this finite element model: flange plate, pad holder, pad sample, disc sample (T-h-4-2 surface) and rotational table. For the contact pairs, the disc surface is defined as the master surface and the pad is selected as the slave surface. The disc surface run-out and thermal effects are not taken into account. The material parameters set for all the parts of this model can reflect the real test system. A uniformly distributed pressure is applied on the top surface of the flange plate, where is constrained in the radial (x) and tangential (z) directions with no rotational degrees of freedom. The table is rigidly constrained at the nodes of the screwed holes except in the circumferential direction, in which rotational velocity is imposed.

Complex eigenvalue analysis is performed to verify the reliability of the finite element model and detect the stability of the experimental system. The real parts and imaginary parts of the complex eigenvalues represent the level of squeal propensity and the unstable vibration frequencies, respectively. The system will become unstable and show a strong tendency to generate squeal when positive real parts occurs. More information about this method can be found in references [32-34]. Fig. 12 plots the imaginary parts of complex eigenvalue with the friction coefficient varying from 0 to 0.5. Two adjacent modes (the 7^{th} and 8^{th} modes) are found to merge together and consequently form an unstable complex mode at the frequency of about 1205 Hz when friction coefficient increases to 0.13. The unstable mode shows that the main vibration occurs in the pad subsystem, which consists of the pad holder carrying pad sample sliding to the rim of disc surface. The unstable frequency of 1205 Hz calculated is very close to the experimental squeal frequency of 1175 Hz, and thus this finite element model can well reflect the dynamic behaviour of the experimental system.

It has been reported that the contact pressure distributions of interface is able to affect the stability of friction system, and squeal noise is usually caused by the non-uniform pressure distribution. The squeal can be excited when the leading edge and leading point of pad surface become the main area of contact pressure concentration [12, 35-36]. Considering that the pressure distributions at the interface would change when the grooves pass through the pad surface, the pressure distributions of the contact surfaces at different contact states are analysed, to shed light on the ability of grooved surface in reducing squeal generation. The leading edge and leading point of pad surface are defined and illustrated in Fig. 13.

The pressure distributions of the contact surfaces in the first half cycle of pad-on-grooved surface are analysed, and some contact states during the friction process and the corresponding pressure distributions are summarized, as shown in Fig. 14(a). The grooves

are found to effectively interrupt and transfer the distribution of contact pressure during sliding, and the highest pressure (red part) of pad surface changes location constantly and is not concentrated at one area. This indicates that the grooves can create a favourable contact pressure distribution to suppress the squeal generation. However, the pressure distributions observed in the second half cycle of pad-on-smooth surface is significantly different from those in the first half cycle, as shown in Fig. 14(b). In the first half cycle, the highest contact pressure always occurs at the edge of a groove because of stress concentration at a geometric discontinuity. In the real disc samples, the groove edges are not at a right angle and thus the true pressure is not as big as predicted by the numerical analysis. In contrast, in the second half cycle, the highest contact pressure often occurs away from a groove edge. A high contact pressure (and thus high pressure gradient) is known to be helpful to squeal generation [15, 36-37].

4.3.2 Effect of groove parameters on squeal generation

The parameters of grooves are found to affect the squeal generation, and the different grooved surfaces show different performances in squeal reduction. The variation of the groove parameters presented above may cause partial loss of contact area, which would consequently result in the variation of the local contact stiffness. Accordingly, a single particle mass model which possesses exactly two modes of vibration in the normal and tangential directions is formulated in Fig. 15, to investigate the effect of contact stiffness on squeal instability of the friction system. The creation of this simplified model is meant to provide a plausible explanation to the experimental phenomenon under this investigation and try to explore how the variation of grooves parameters affects the squeal instability through changing the contact stiffness, and is not intended to reproduce the experimental results [38]. So the parameters of this model used in the simulation are not made to fit the true parameter values of the friction system of Fig. 1.

A conveyor belt travelling at a constant velocity is loaded by a constant normal force N applied to the mass. The mass is held by two linear springs, which are denoted by K_1 and K_2. In addition, the physical contact stiffness between the mass and the belt in relative sliding motion is modelled by a spring K_{n} for the normal component. For the friction law, a Coulomb-type friction force $F_f = \mu F_n$ with a constant kinetic friction coefficient μ, is assumed.

As damping is very small in the friction system of Fig. 1, it can be ignored for simplicity. The linear spring K_2 is mounted at oblique angle θ of 45°, the dynamics equations of the

model can be written as follows:

$$\begin{bmatrix} m & 0 \\ 0 & m \end{bmatrix}\begin{pmatrix} \ddot{x} \\ \ddot{y} \end{pmatrix}+\begin{bmatrix} K_1+\frac{1}{2}k_2 & -\frac{1}{2}K_2+K_n\mu \\ -\frac{1}{2}K_2 & \frac{1}{2}K_2+K_n \end{bmatrix}\begin{pmatrix} x \\ y \end{pmatrix}=\begin{pmatrix} 0 \\ N \end{pmatrix} \quad [1]$$

The stiffness matrix in Eq. (1) is asymmetric because of the friction effects, thus this system has complex eigenvalues when the parameters are at certain values. According to vibration theory, the response of the model can be expressed by $u_i = A_i e^{\lambda t} = A_i e^{(a+bi)t}$, where the positive real parts and the imaginary parts of the exponential term represent the degrees of instability and the frequencies of the corresponding modes, respectively. Setting m=1 kg, K_1=5×10^5 N/m, K_2=4×10^5 N/m.

Fig. 16 shows the mode coalescence of the model. It is found that two separated surfaces start to merge into a relatively flat one, with the normal contact stiffness and friction coefficient increasing to a certain value, indicating that the two adjacent modes tend to form an unstable complex mode (Fig. 16(a)). In this condition, the single surface of the real parts start to bifurcate into a positive-valued surface and a symmetric negative-valued surface, which suggests that the displacement response u_i will increase with time and the two-degrees-of-freedom model becomes unstable, indicating the friction system has a strong propensity to generate unstable vibration (Fig. 16 (b)).

The transient dynamic behaviour of the model versus time is calculated by using Runge-Kutta method, and the results are shown in Fig. 17. A friction coefficient of 0.4 is set, the system is found to be stable at a low value of normal contact stiffness of 2.5×10^5 N/m. When the normal contact stiffness increases to a higher value of 5×10^5 N/m, a significant continuous high-frequency fluctuation with exponential growth is observed. This indicates that the model becomes unstable and generates squeal noise in a relatively high value of contact stiffness. As the surface region with wider grooves would result in a reduction of local contact stiffness, it can be concluded that such a surface feature would lead to better performance in reducing squeal generation.

5. Conclusions

In this work, disc surface modifications in the form of parallel and radial grooves have been tested with respect to the noise reduction properties. Moreover, a customised disc sample with parallel grooves made on only half of its surface is tested to further demonstrate the capability of grooved surface in reducing squeal noise generation. In addition, a numerical study of the vibration behaviour of the friction system is performed to provide a possible

explanation for the experimental phenomenon. The conclusions are summarized as follows:

(1) The disc surface topography with grooved modifications shows a good performance in reducing squeal noise. Moreover, the configurations of grooves have effect on the vibration and noise characteristics of contact surface. The level of vibration and noise is found to decrease with increasing groove width for both kinds of the disc surfaces having parallel and radial grooves.

(2) For the disc sample with parallel grooves on only half of its surface, it is found that grooves on the contact surface can reduce the energy density contained in the excited frequencies and thus suppress the squeal noise generation of the friction system. Moreover, the grooves are found to be able to play a storage cavity role in trapping wear debris and change the wear features of the disc surface.

(3) The numerical results of the detailed finite element model show that the grooves on the disc surface is able to affect the contact pressure distribution of the pad surface during the friction process, and redistribute the concentrated interface pressure and consequently suppress squeal generation. In addition, the effect of the local contact stiffness of a simplified two-degree-of-freedom model on its dynamic instability is studied, which may help explain why disc samples with different groove parameters have different abilities in reducing squeal noise generation.

6. Acknowledgements

The authors would like to thank Professor G.X. Chen and M.H. Zhu of Southwest Jiaotong University, for helpful discussions. The authors are grateful for the financial support of the National Natural Science Foundation of China (No. 51375408), and the Program for New Century Excellent Talents in University (NCET-13-0974). The fourth author is grateful to the travel grant provided in the form of Changjiang Scholar Professorship.

Reference

[1] A. Akay, Acoustics of friction, J. Acoust. Soc. Am. 114 (2002) 1525-1548.

[2] A. Papinniemi, J.C.S. Lai, J.Y. Zhao, L. Loader, Brake squeal: a literature review, Appl Acoust. 63 (2002) 391-400.

[3] F. Chen, Automotive disk brake squeal: an overview, Int. J. Veh. Des. 51 (1/2) (2009) 39-72.

[4] N.M. Kinkaid, O.M. O'Reilly, P. Papadopoulos, Automotive disc brake squeal, J. Sound Vib. 267 (2003) 105-166.

[5] H.R. Mills, Brake squeak, Technical Report 9000 B, Institution of Automobile Engineers, 1938.

[6] R.T. Spurr, A theory of brake squeal, Proc. Automot Div Inst Mech Eng 1961-1962 (1) (1961) 33-52.

[7] M.R. North, Disc brake squeal, Proc. Inst. Mech. Eng. C38/76 (1976) 169-176.

[8] H. Ouyang, J.E. Mottershead, W. Li, A moving-load model for disc-brake stability analysis, ASME J. Vib. Acoust. 125 (1) (2003) 1-6.

[9] M. Graf, G.-P. Ostermeyer, Friction-induced vibration and dynamic friction laws: Instability at positive friction-velocity-characteristic, Tribol Int. 92 (2015) 255-258.

[10] S. Oberst, J. Lai, A critical review of brake squeal and its treatment in practice, Internoise 2008, Shanghai, 2008.

[11] M. Eriksson, F. Bergman, S. Jacobson, Surface characterisation of brake pads after running under silent and squealing conditions, Wear 232 (1999) 163-167.

[12] M. Eriksson, F. Bergman, S. Jacobson, On the nature of tribological contact in automotive brakes, Wear 252 (2002) 26-36.

[13] F. Bergman, M. Eriksson, S. Jacobson, Influence of disc topography on generation of brake squeal, Wear 225-229 (1999) 621-628.

[14] L. Hammerström, S. Jacobson, Surface modification of brake discs to reduce squeal problems, Wear 261 (2006) 53-57.

[15] A.R. AbuBakar, H. Ouyang, S. James, L Li. Finite element analysis of wear and its effect on squeal generation. Proceedings of the Institution of Mechanical Engineers, Part D: Journal of Automobile Engineering 222 (208) 1153-1165.

[16] M.W. Shin, Y.H. Kim, H. Jang. Effect of the abrasive size on the friction effectiveness and instability of brake friction materials: a case study with zircon, Tribol Lett 55 (2014) 371-379.

[17] H. Hetzler, K. Willner. On the influence of contact tribology on brake squeal, Tribol Int. 46(1) (2012) 237-246.

[18] S.W. Yoon, M.W. Shin, W.G. Lee, H. Jang, Effect of surface contact conditions on the stick-slip behaviour of brake friction material, Wear 294-295 (2012) 305-312.

[19] S.M. Lee, M.W. Shin, W.K. Lee, H. Jang, The correlation between contact stiffness and stick-slip of brake friction materials, Wear 302 (2013) 1414-1420.

[20] A. R. M. Lazim, M. K. A. Hamid, A. R. AbuBakar, Effects of pad surface topography on disc brake squeal, App. Mech. Mat. 165 (2012) 58-62.

[21] V. Magnier, J.F. Brunel, P. Dufrénoy, Impact of contact stiffness heterogeneities on friction-induced vibration, Int. J. Solids Struct. 51 (2014) 1662-1669.

[22] P. Duffour, J. Woodhouse. Instability of systems with a frictional point contact. Part 3: experimental tests. J. Sound Vib. 304 (2007)186-200.

[23] T. Butlin, J. Woodhouse. A systematic experimental study of squeal initiation. J. Sound Vib. 330(21) (2011) 5077-5095.

[24] S. Oberst, J.C.S. Lai, Statistical analysis of brake squeal noise, J. Sound Vib. 330 (2011) 2978-2994.

[25] C.L. Saw, C.G. Choong, A.R. AbuBakar, M.R. Jamaluddin, W.M.M.W. Harujan, B.A. Ghani, Disc brake squeal suppression through chamfered and slotted pad, International Int. J. Vehicle Struct. Syst. 3(1) (2011) 28-35.

[26] J.L. Mo, Z.G. Wang, G.X. Chen, T.M. Shao, M.H. Zhu, Z.R. Zhou, The effect of groove-textured surface on friction and wear and friction-induced vibration and noise, Wear 301 (2013) 671-681.

[27] W. Tang, Y.K. Zhou, H. Zhu, H.F. Yang. The effect of surface texturing on reducing the friction and wear of steel under lubricated sliding contact. Appl. Surf. Sci. 273 (2013) 199-204.

[28] I. Etsion, Improving tribological performance of mechanical components by laser surface texturing, Tribol T. 17 (2004) 733-737.

[29] A. Erdemir, Review of engineered tribological interfaces for improved boundary lubrication, Tribol Int. 38 (2005) 249-256.

[30] D.Z. Segu, P. Hwang, Friction control by multi-shape textured surface under pin-on-disc test, Tribol Int. 91 (2015) 111-117.

[31] M. Mosleh, B.A. Khemet, A Surface Texturing Approach for Cleaner Disc Brakes, Tribol T. 49 (2006) 279-283.

[32] H. Ouyang, W. Nack, Y. Yuan, F. Chen, Numerical analysis of automotive disc brake squeal: a review, Int. J. Vehicle Noise Vib. 1(3/4) (2005) 207-231.

[33] A.R. AbuBakar, H. Ouyang, A prediction methodology of disk brake squeal using complex eigenvalue analysis, Int. J. Vehicle Des. 46 (2008) 416-435.

[34] A. Bajer, V. Belsay, Combining a nonlinear static analysis and complex eigenvalue extraction in brake squeal simulation, SAE Paper 2003-01-3349.

[35] F. Massi, L. Baillet, O. Giannini, A. Sestieri, Brake squeal: linear and nonlinear numerical approaches, Mech. Syst. Signal Process. 6 (2007) 2374-2393.

[36] A.R. AbuBakar, H. Ouyang, L Li, A combined analysis of heat conduction, contact

pressure and transient vibration of a disk brake, Int. J. Veh. Des. 51 (2009) 190-206.
[37] J.D. Fieldhouse, N. Ashraf, C. Talbot, T. Pasquet, P. Franck, R. Gabriel. Measurement of the dynamic center of pressure of a brake pad during a braking operation. SAE Technical Paper, 2006-01-3208.
[38] D. Hochlenert, G. Spelsberg-Korspeter, P. Hagedorn. A note on safety-relevant vibrations induced by brake squeal, J. Sound Vib. 329 (2010) 3867-3872.

List of figure captions

Fig. 1

Click here to download high resolution image

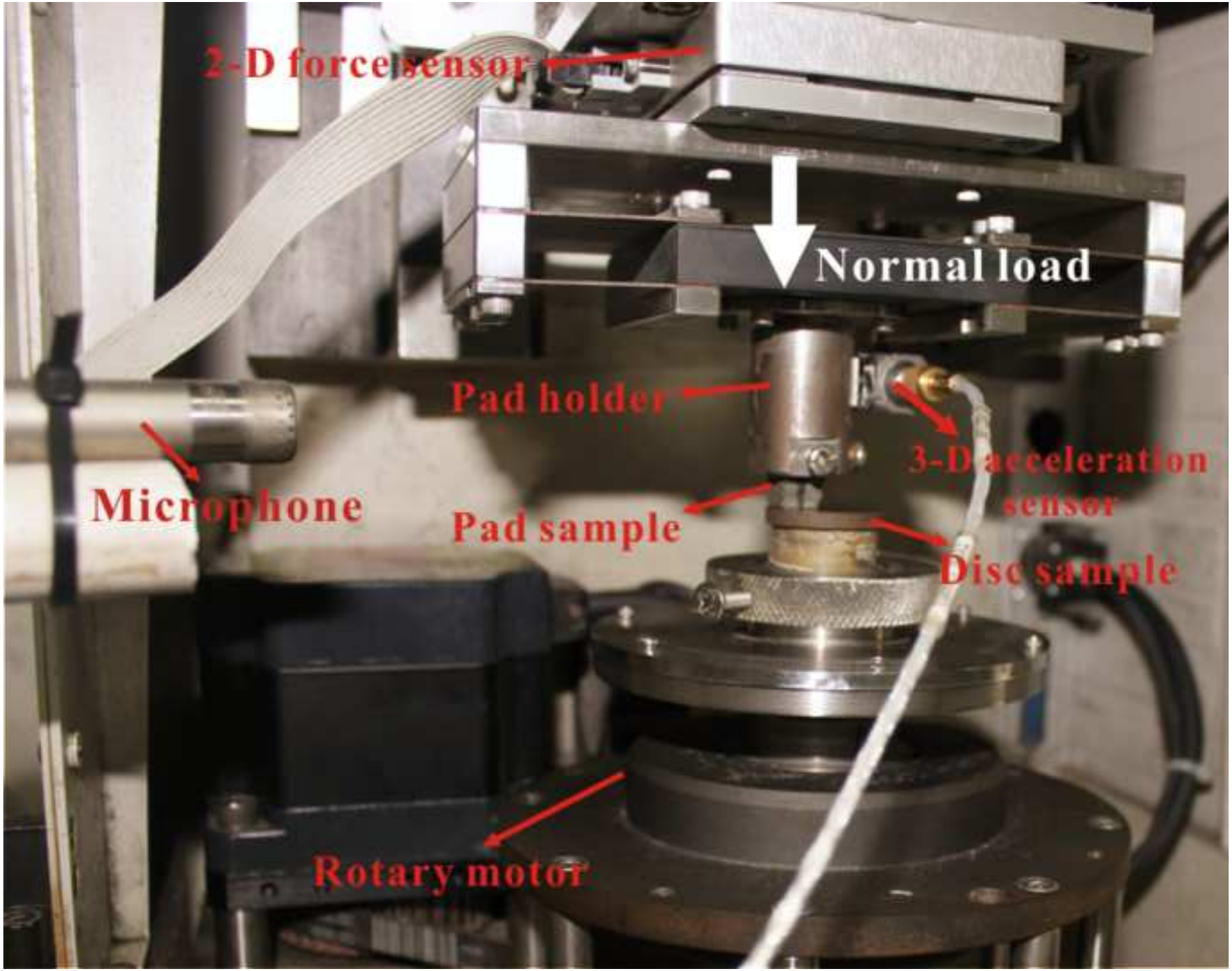

Fig. 2

Click here to download high resolution image

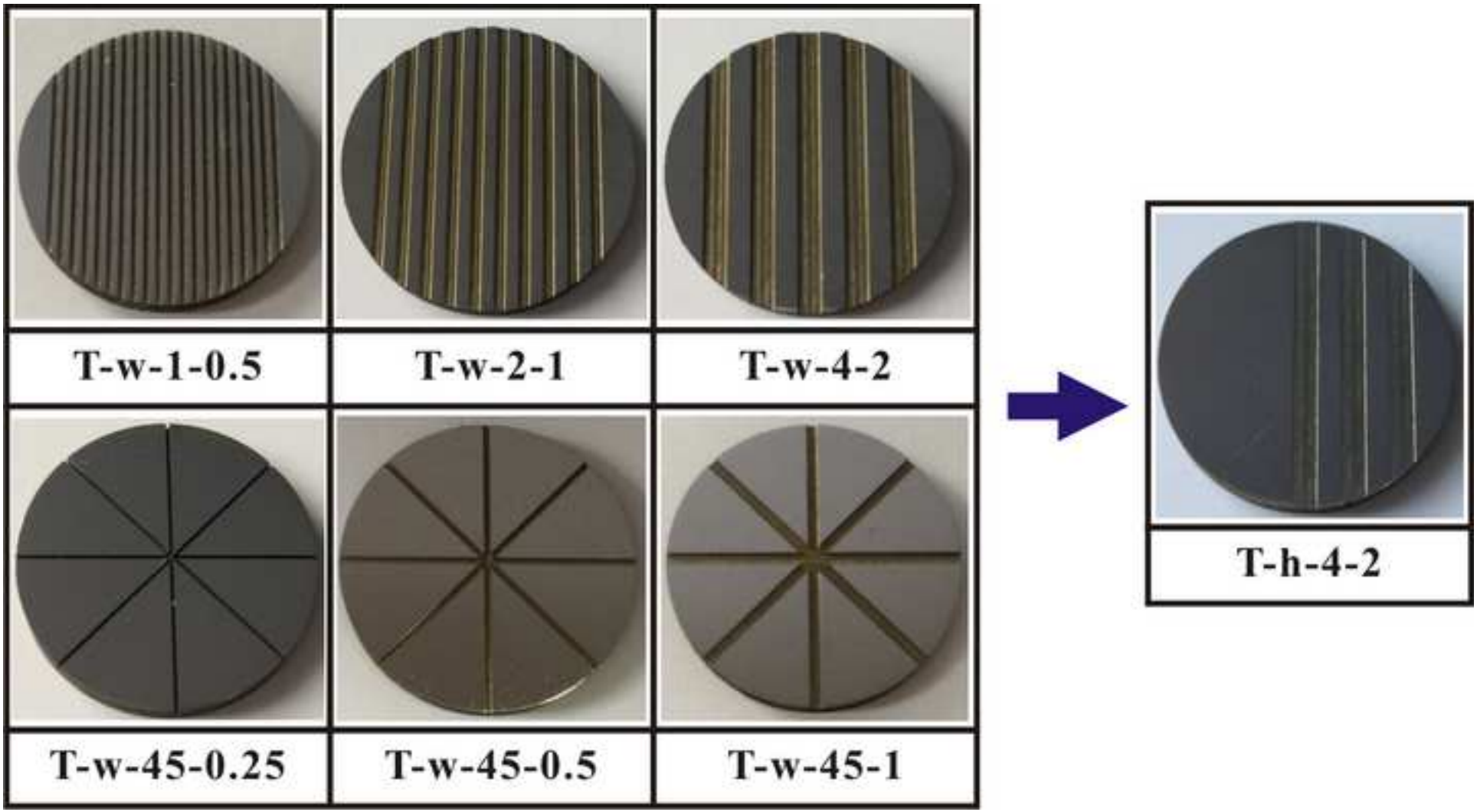

Fig. 3(a)
Click here to download high resolution image

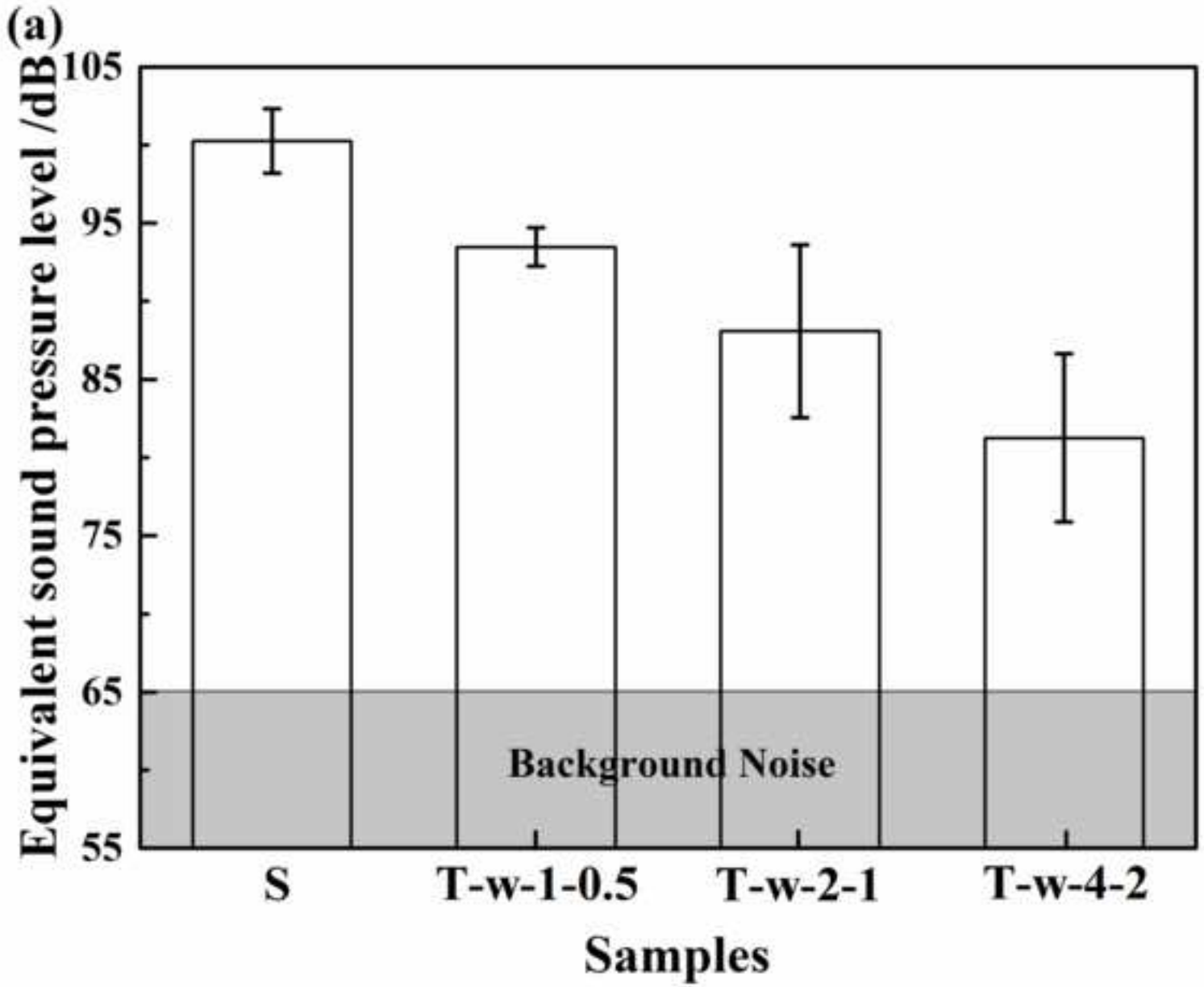

Fig. 3(b)
Click here to download high resolution image

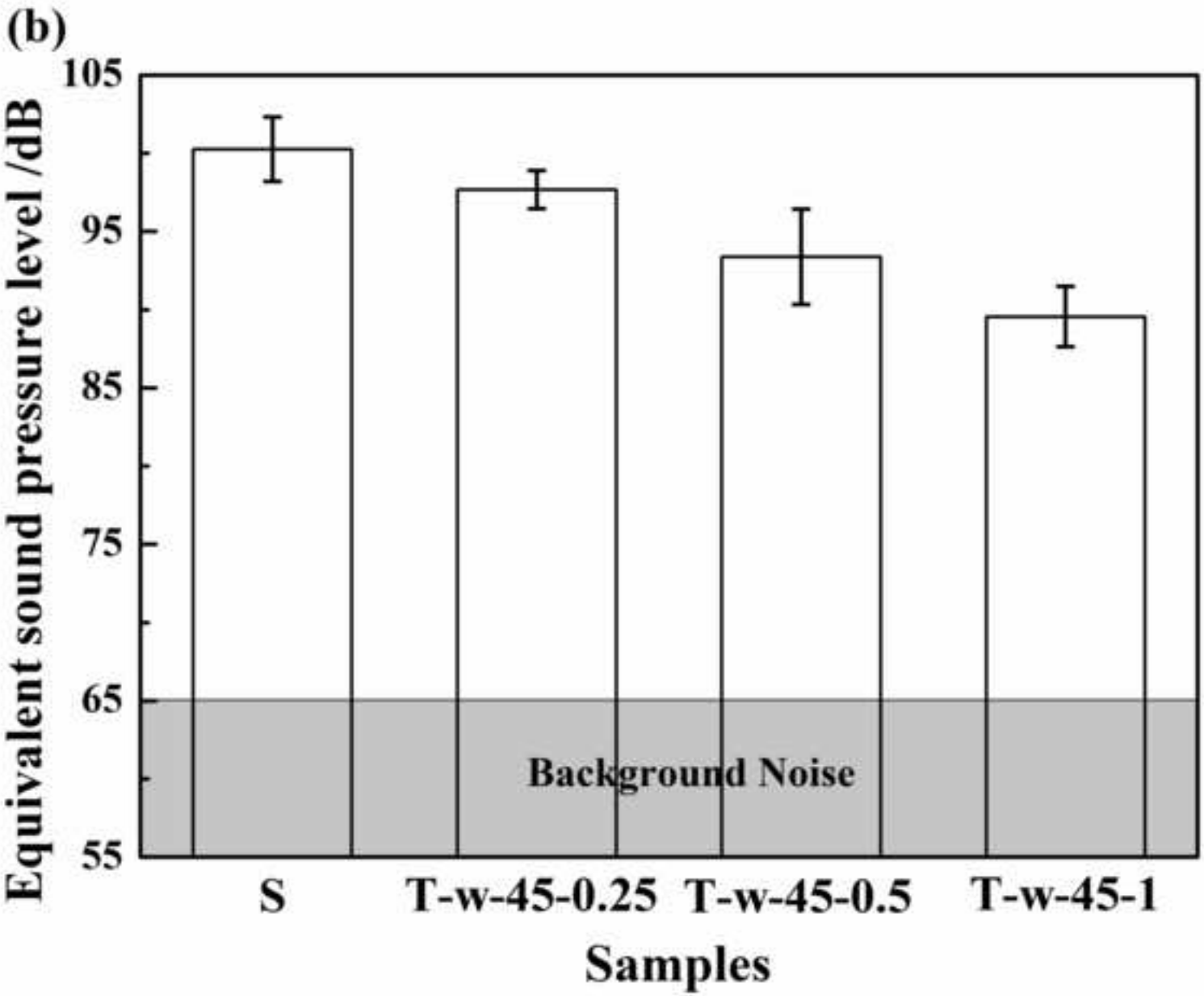

Fig. 4(a)
Click here to download high resolution image

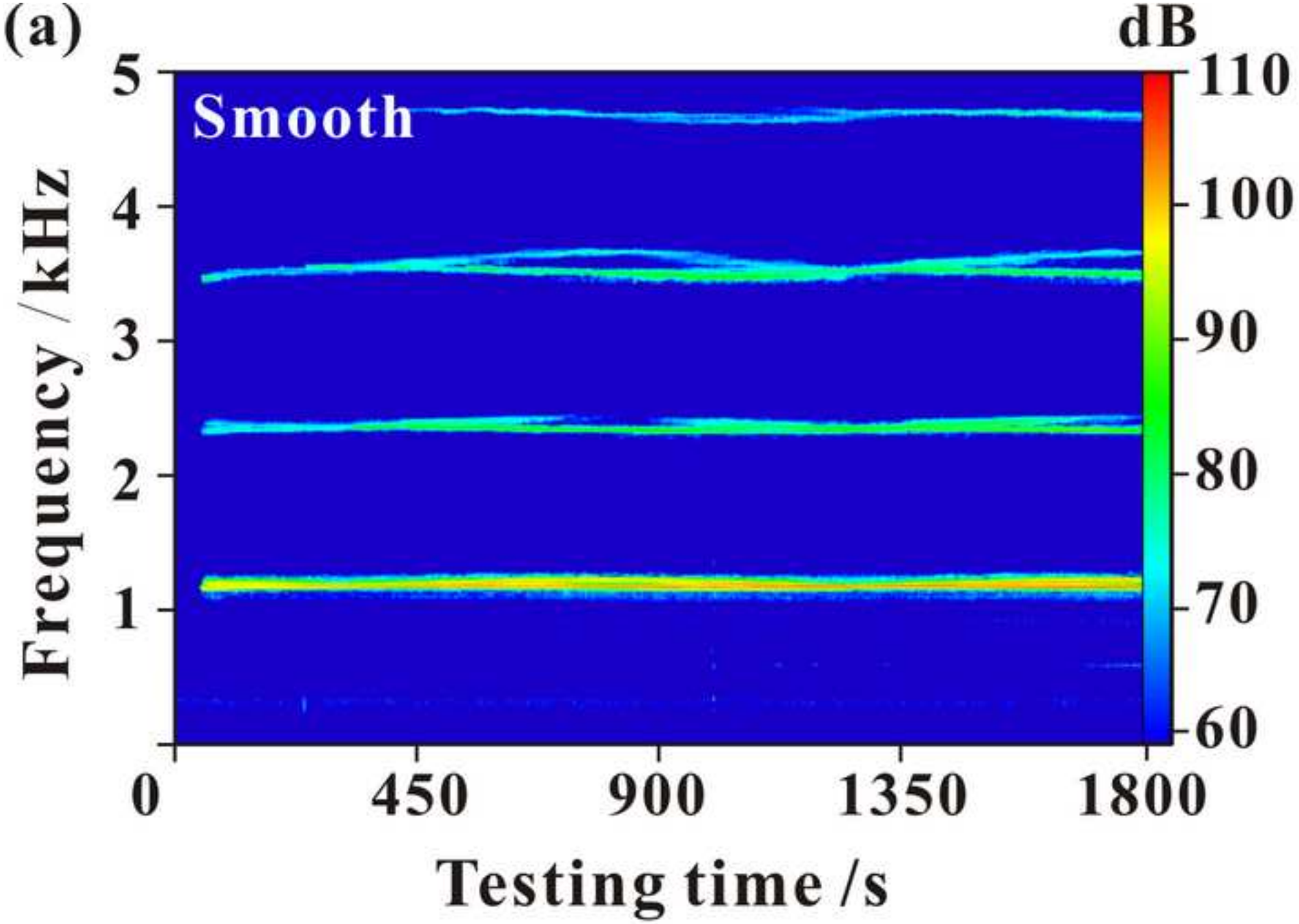

Fig. 4(b)
Click here to download high resolution image

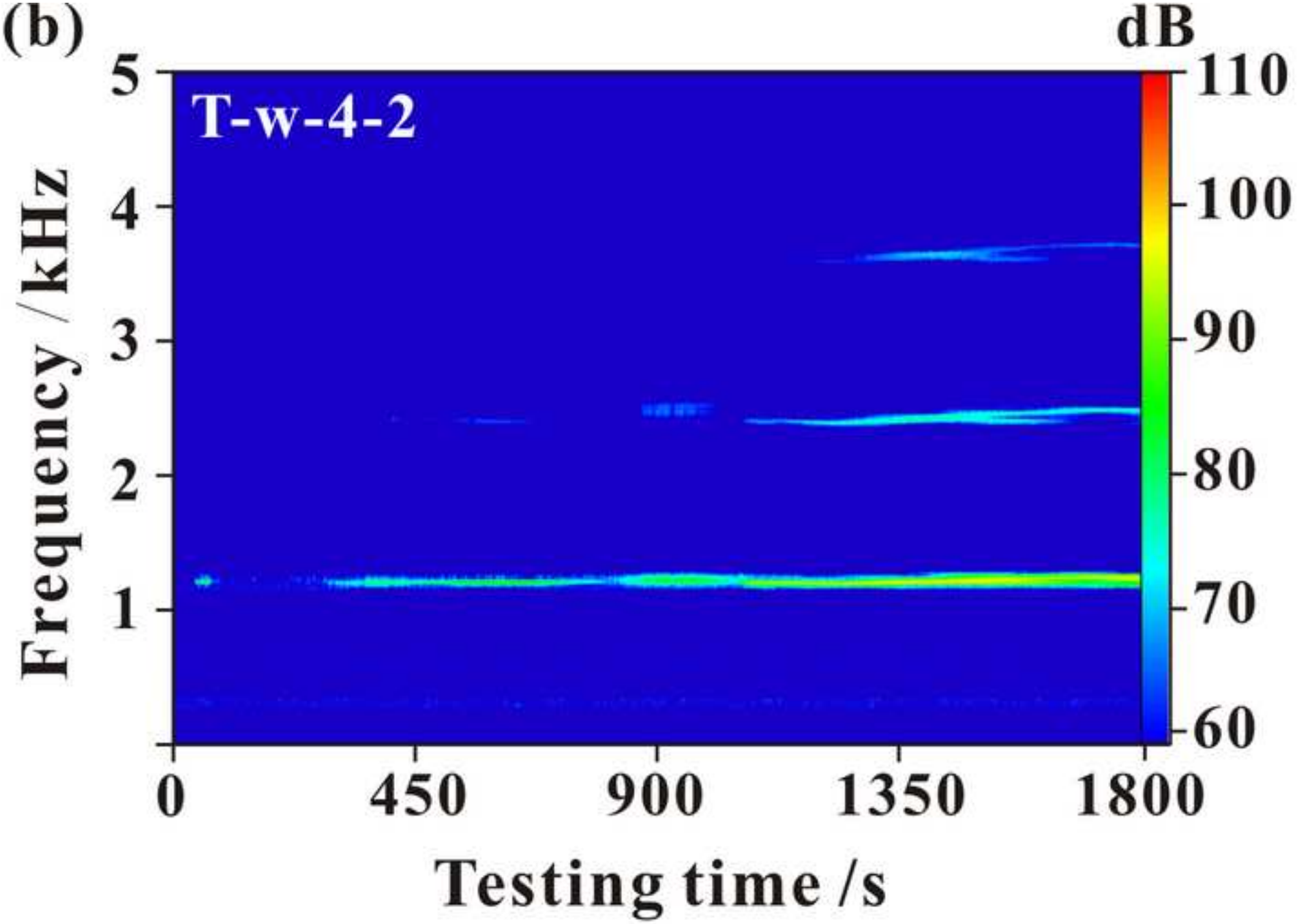

Fig. 4(c)
Click here to download high resolution image

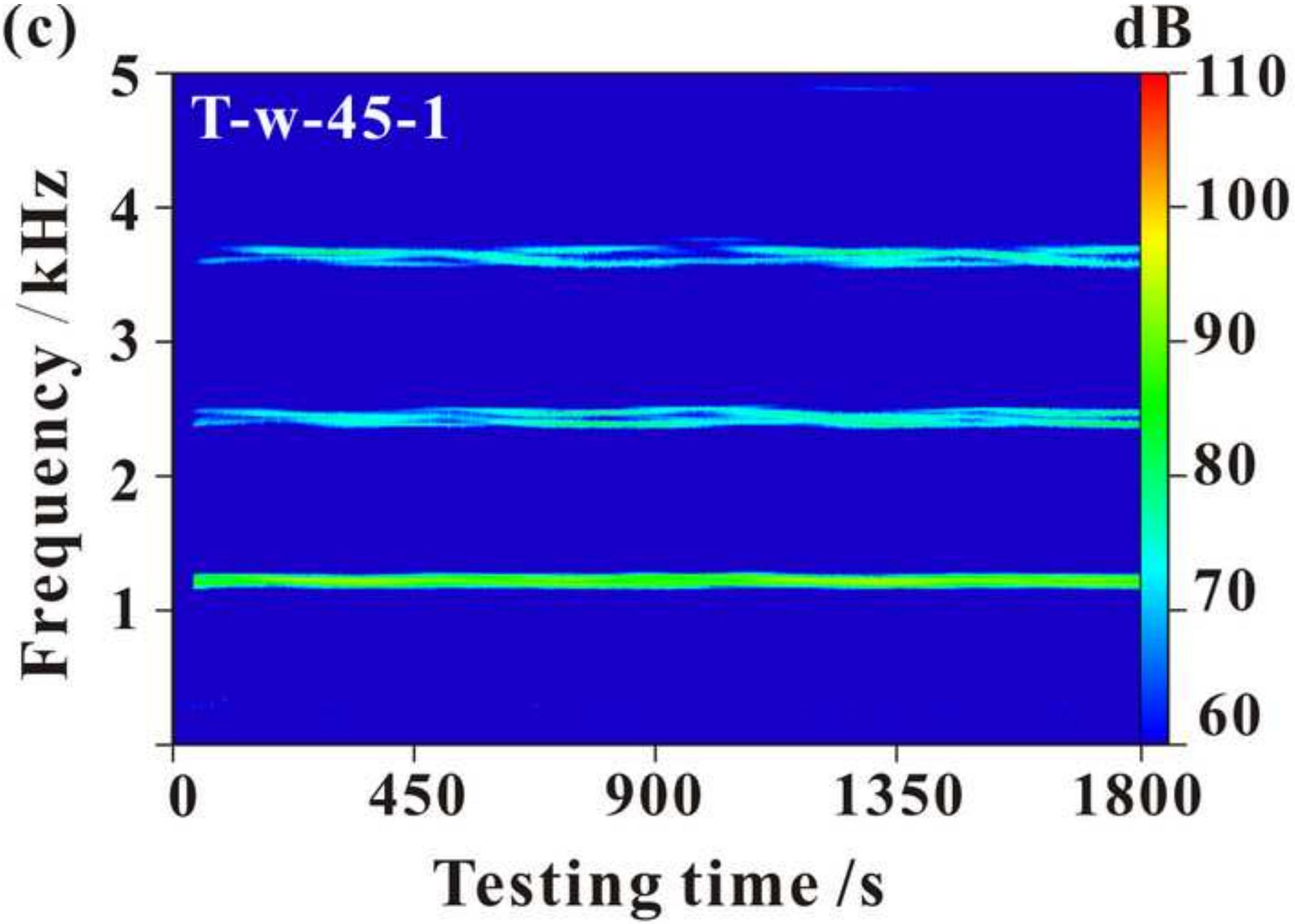

Fig. 5(a)
Click here to download high resolution image

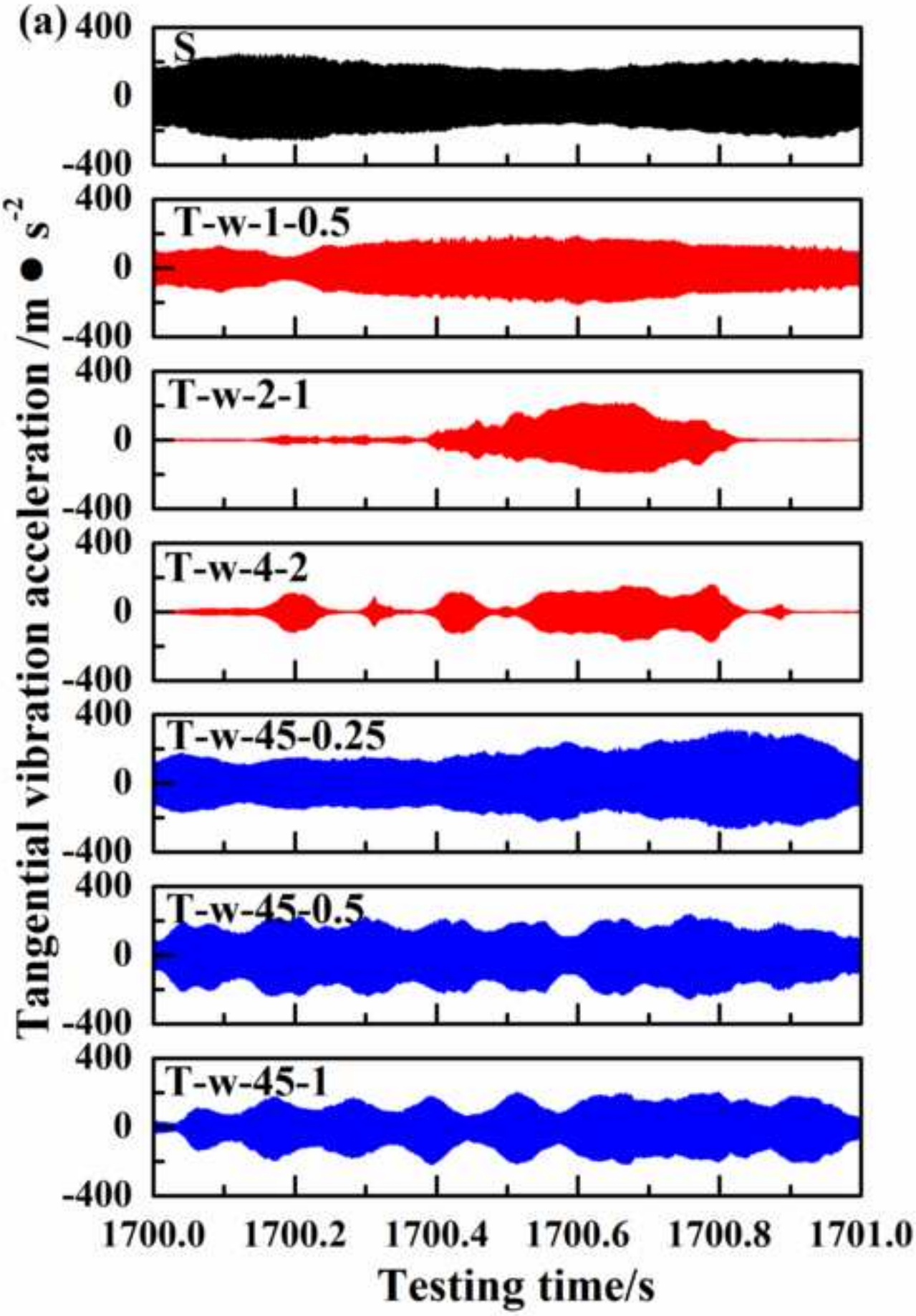

Fig. 5(b)
Click here to download high resolution image

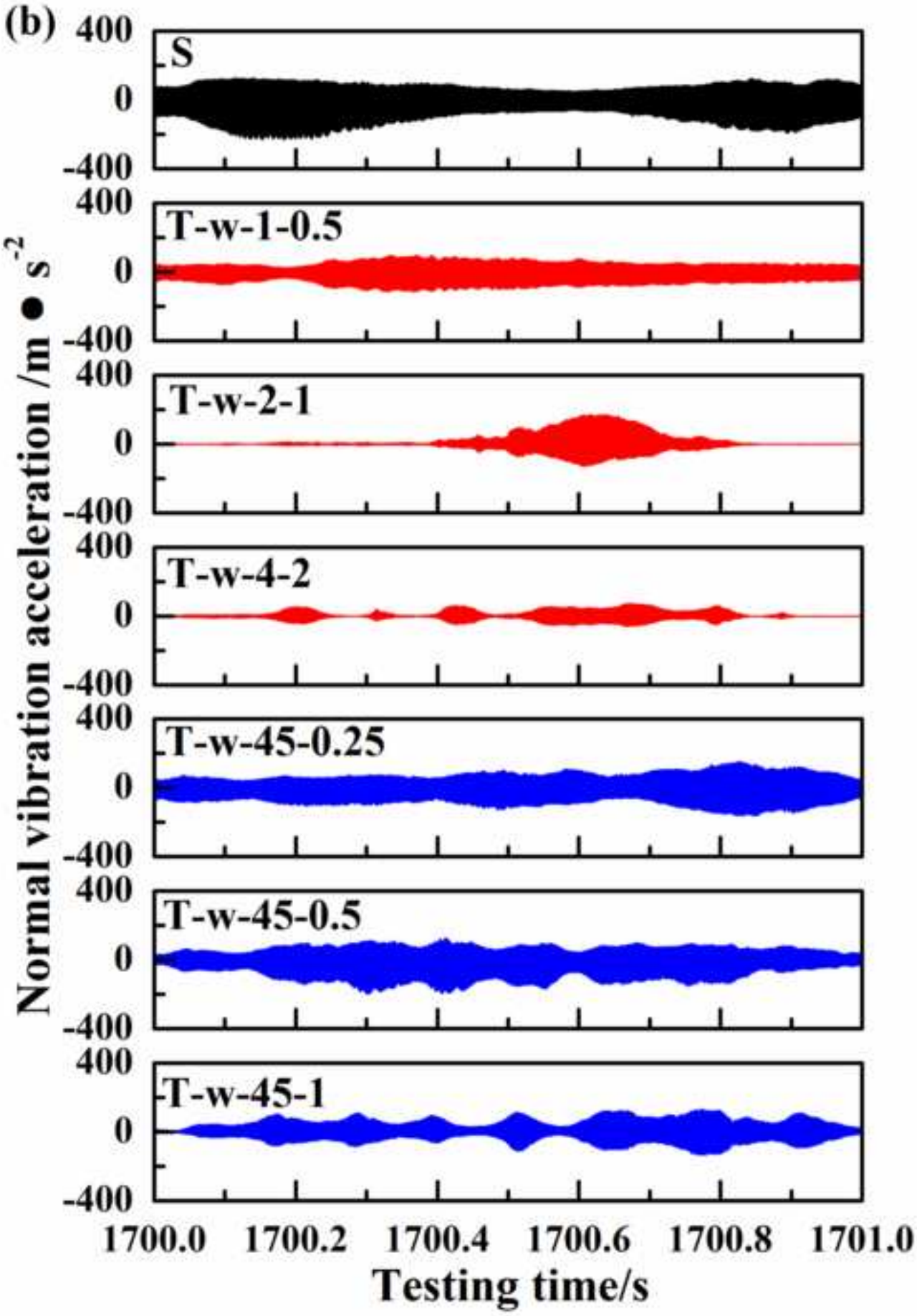

Fig. 5(c)
Click here to download high resolution image

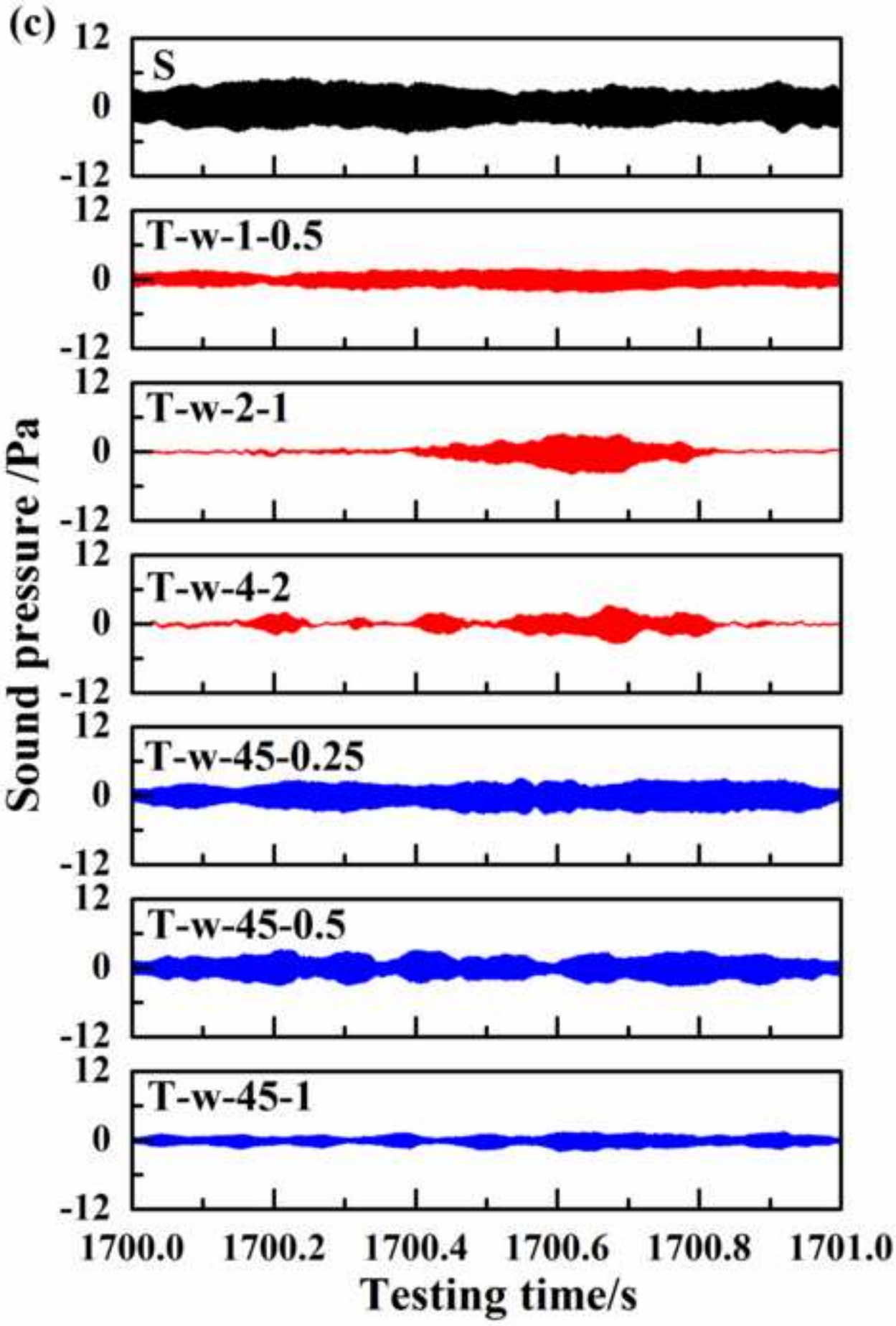

Fig. 6(a)
Click here to download high resolution image

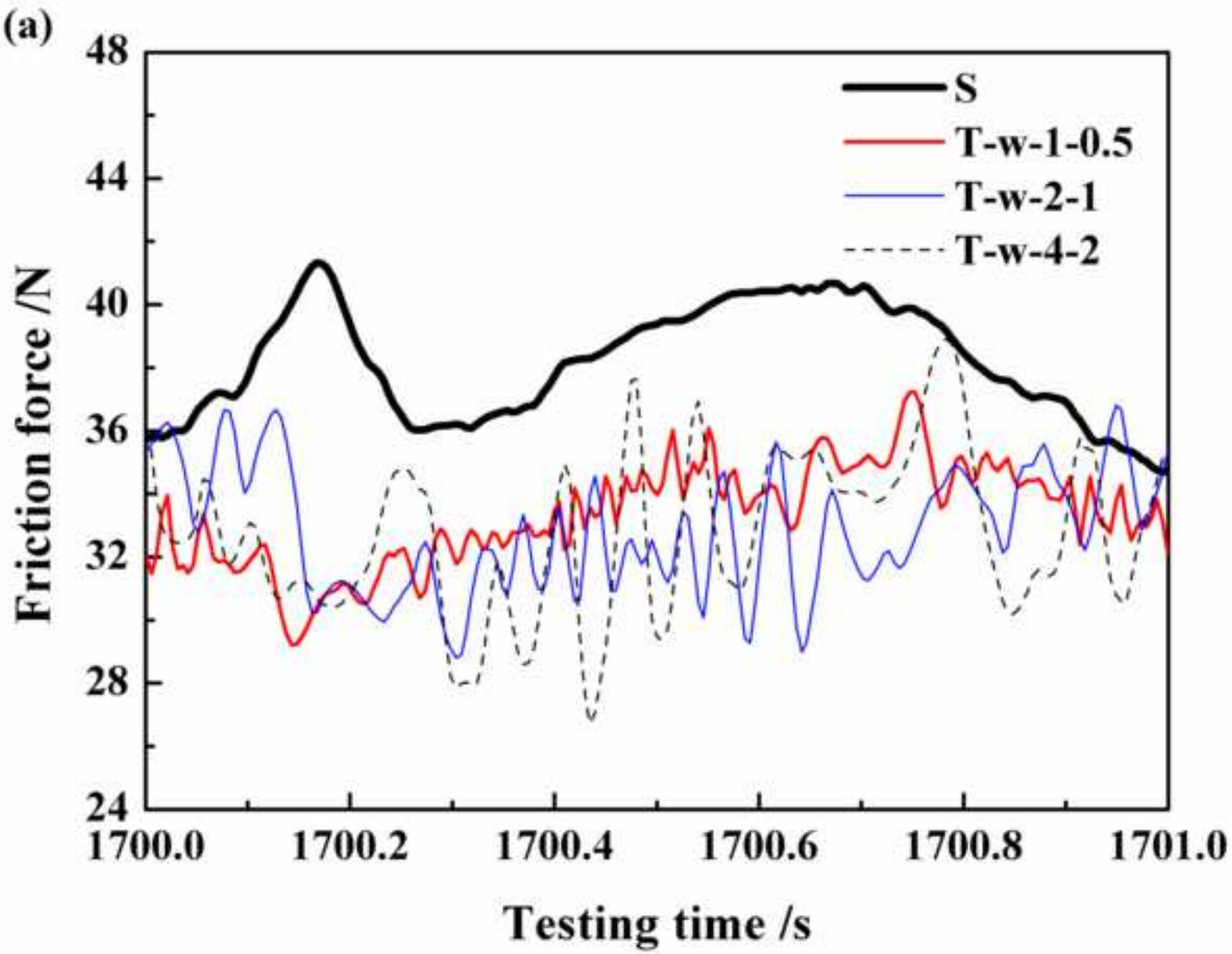

Fig. 6(b)
Click here to download high resolution image

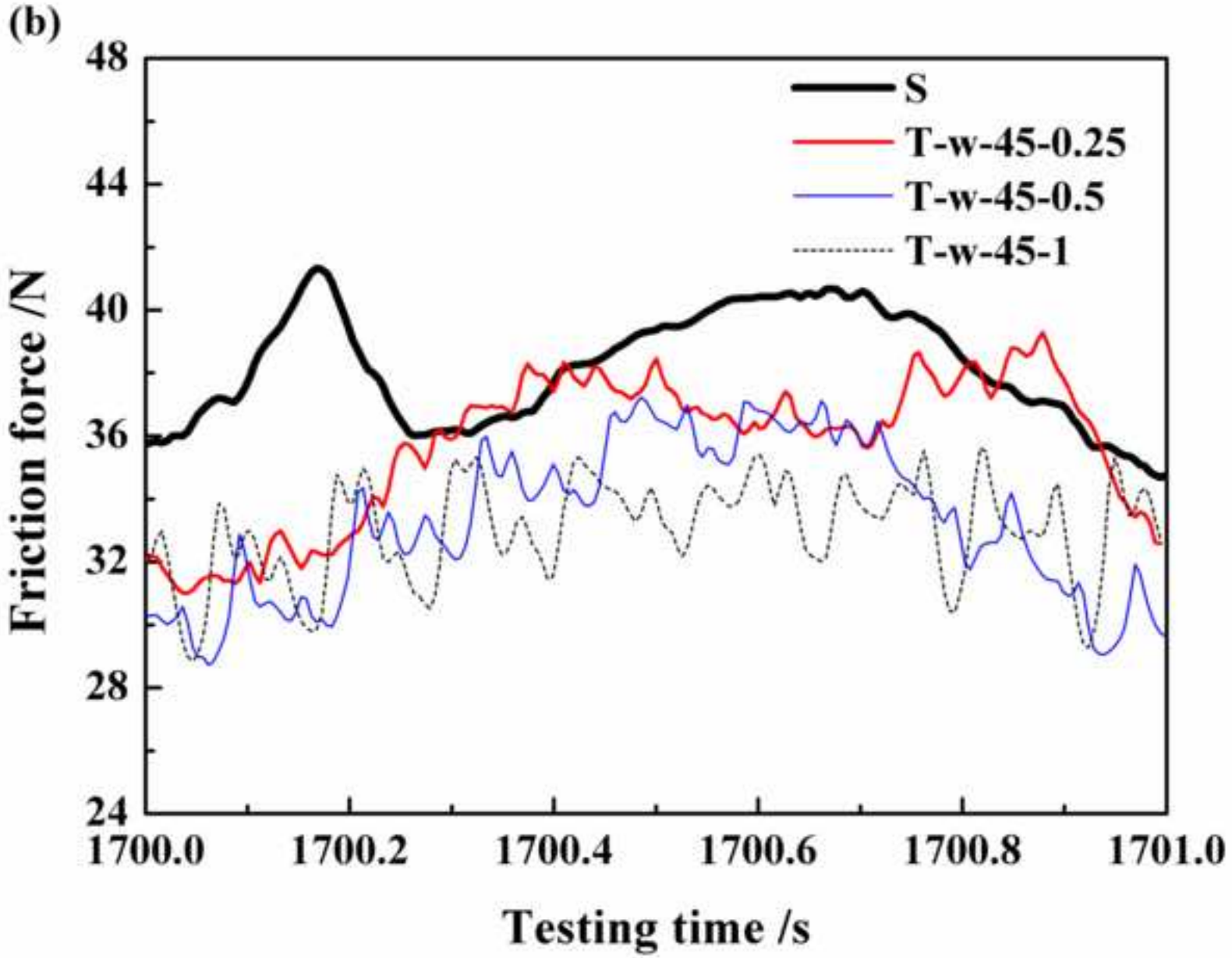

Fig. 7(a)
Click here to download high resolution image

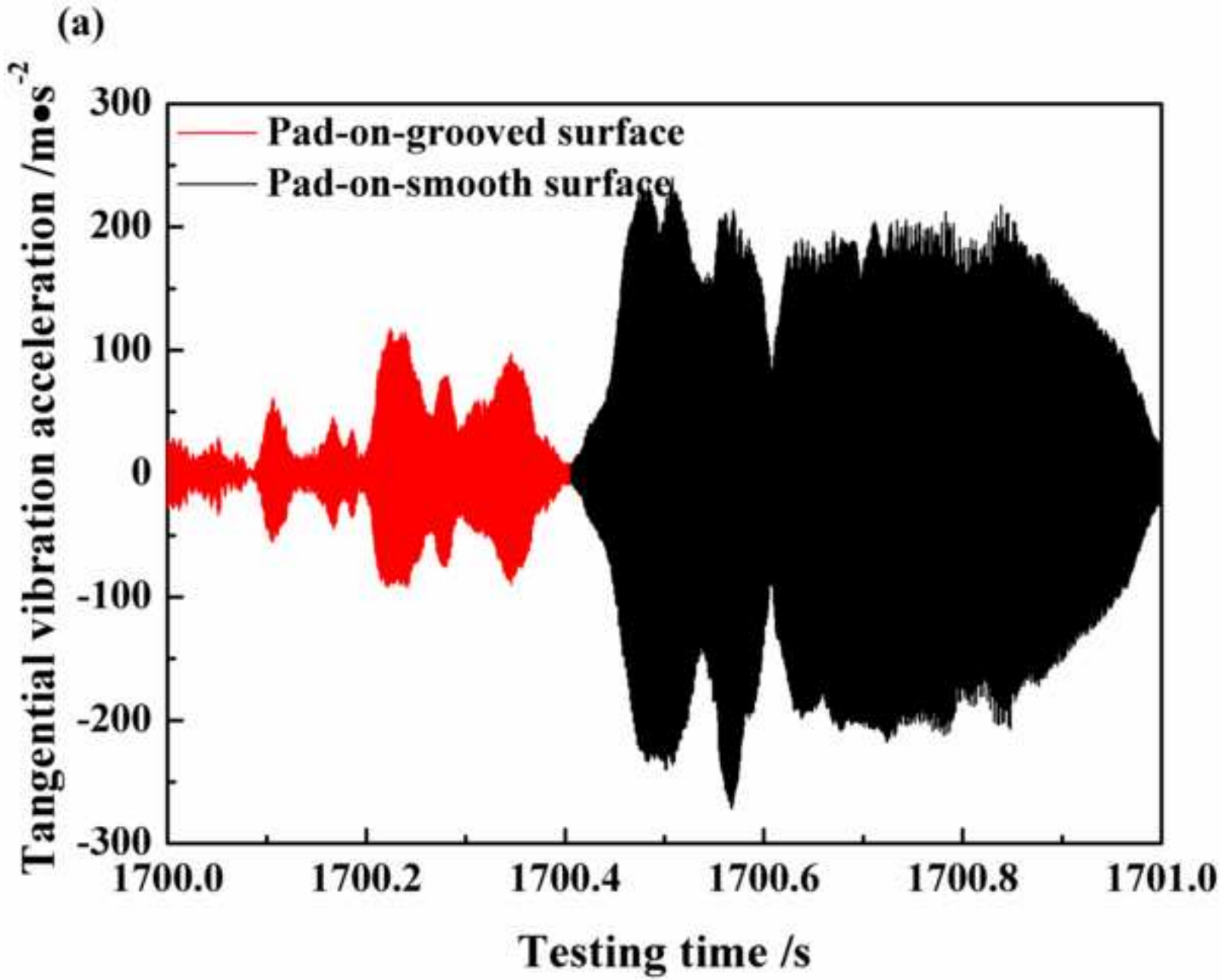

Fig. 7(b)
Click here to download high resolution image

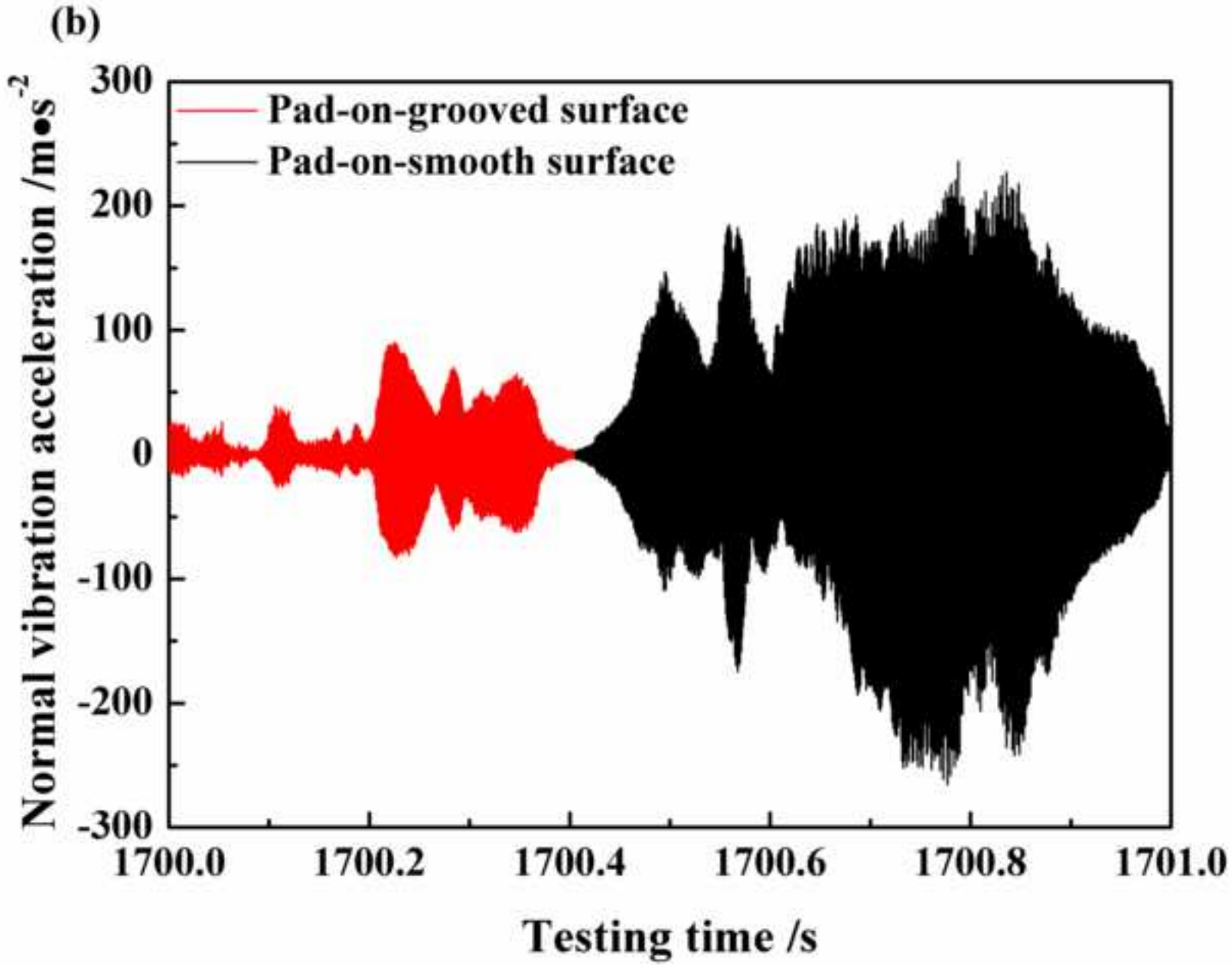

Fig. 7(c)
Click here to download high resolution image

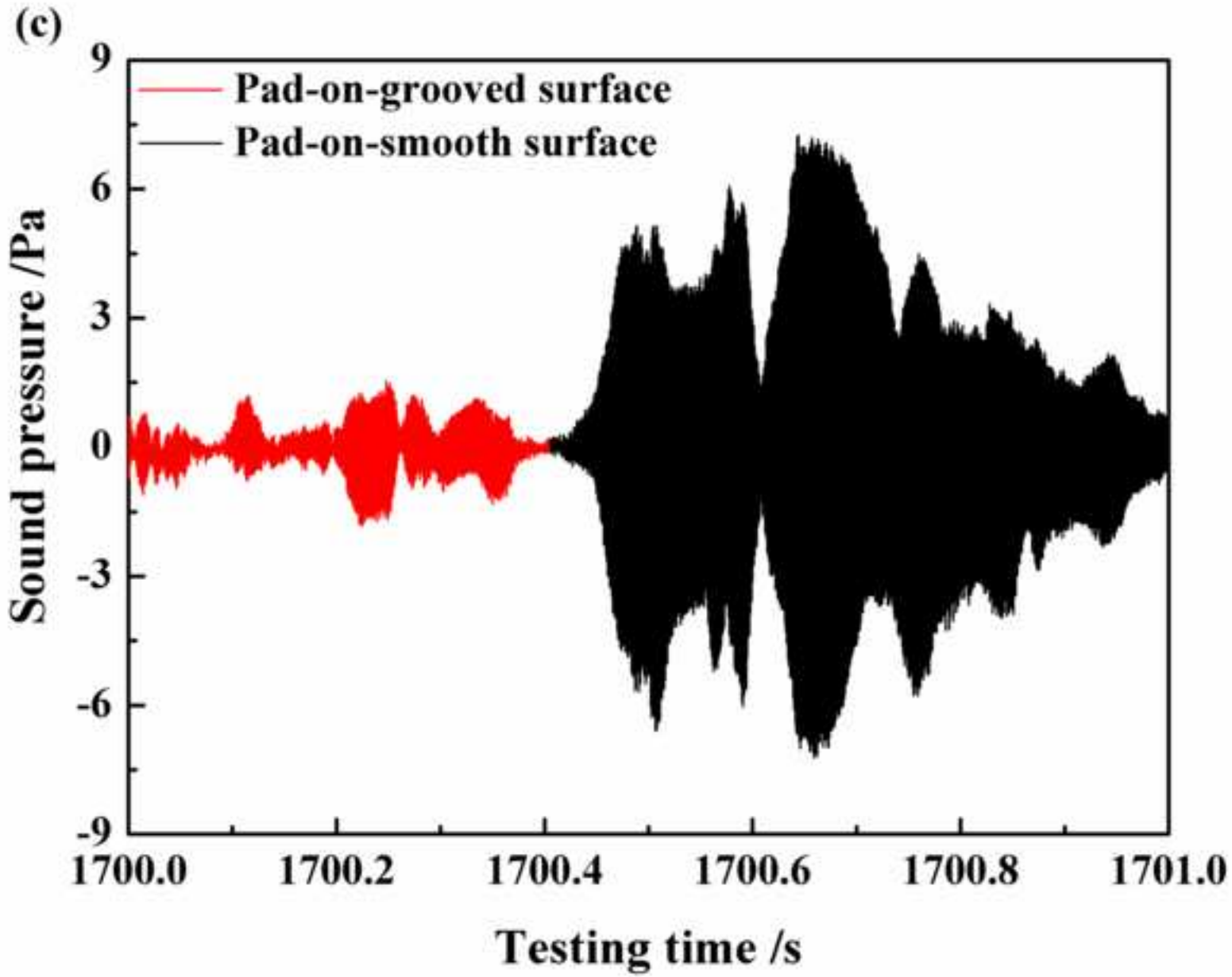

Fig. 7(d)
Click here to download high resolution image

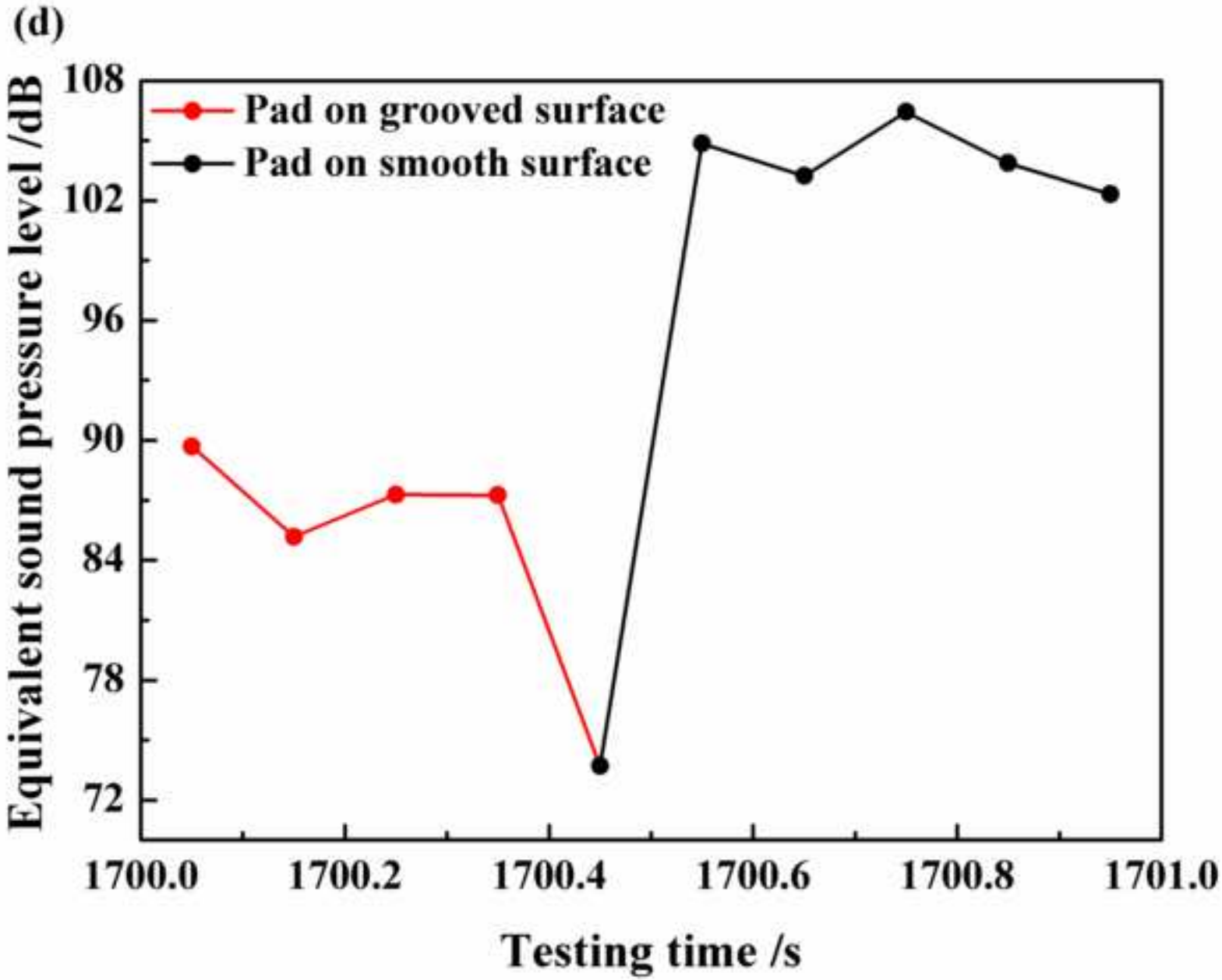

Fig. 8(a)

Click here to download high resolution image

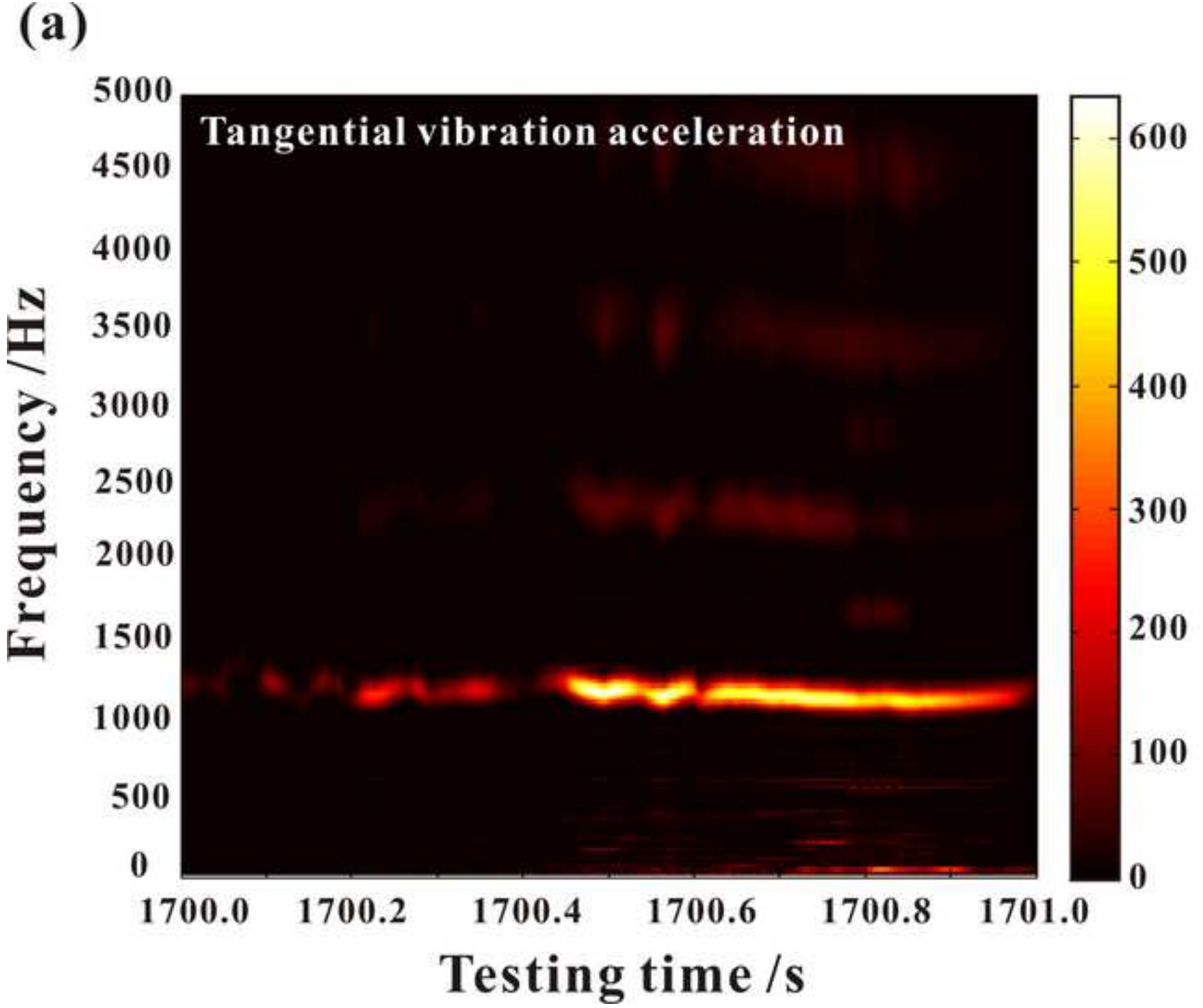

Fig. 8(b)
Click here to download high resolution image

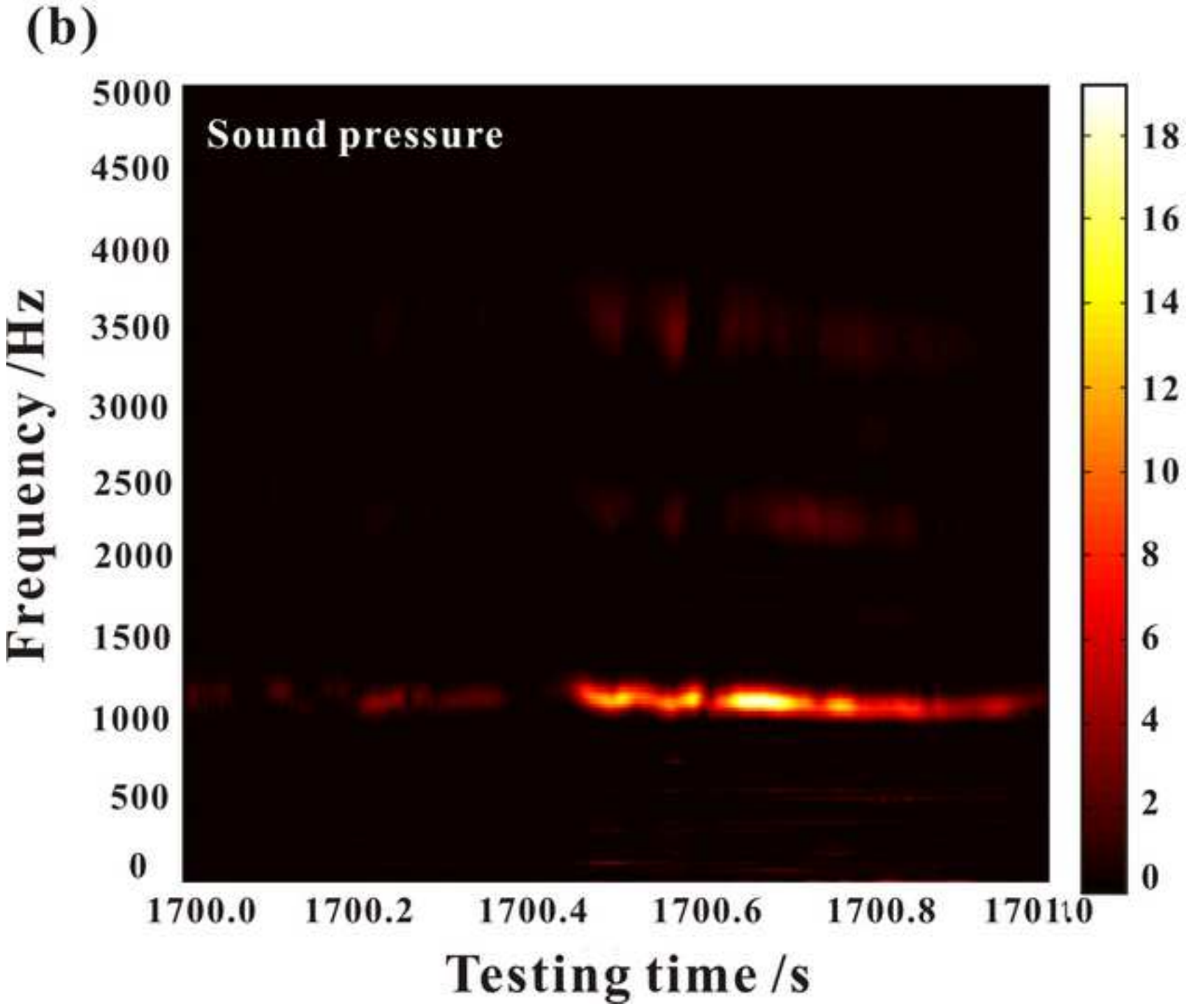

Fig. 9

Click here to download high resolution image

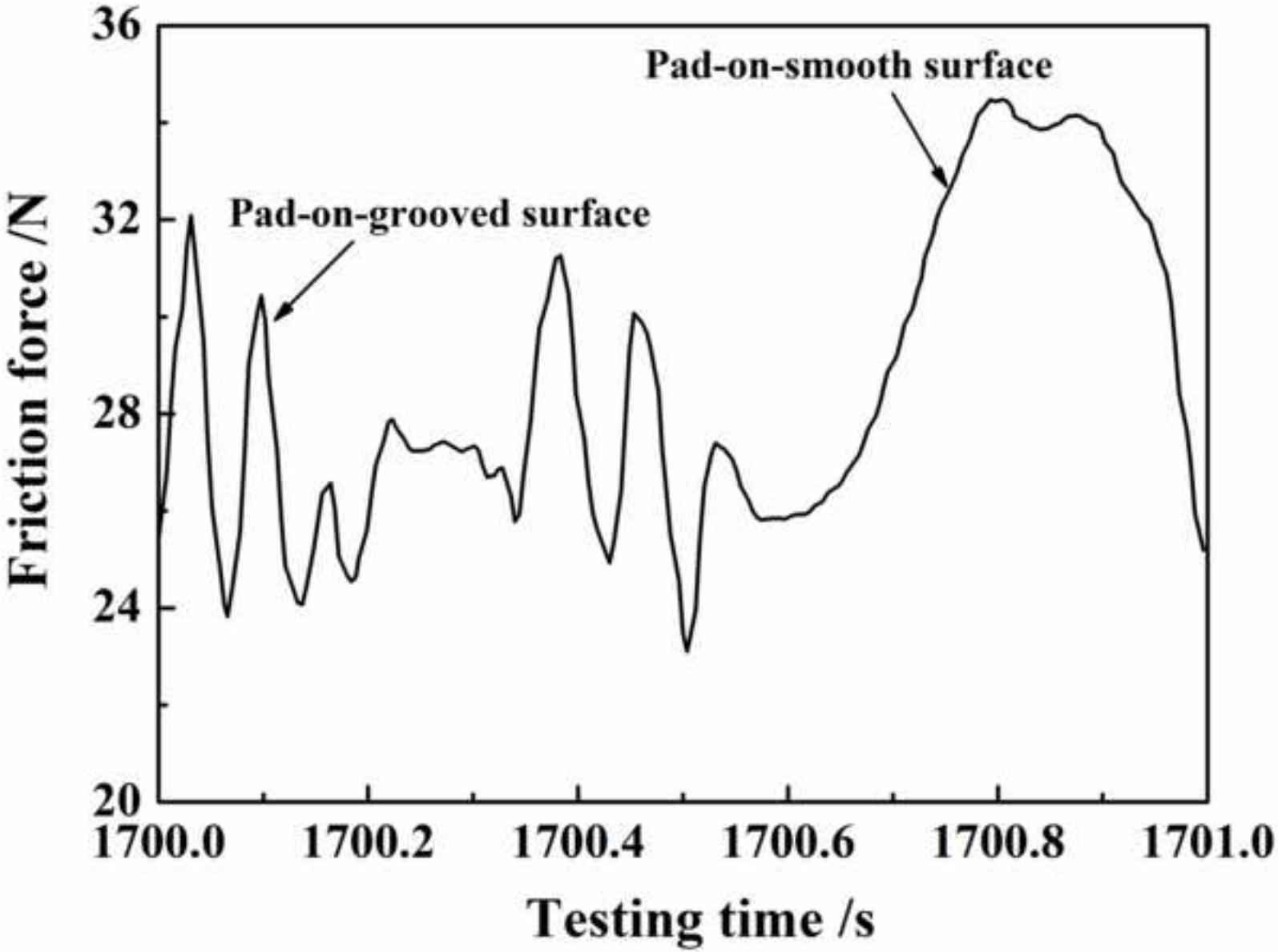

Fig. 10

Click here to download high resolution image

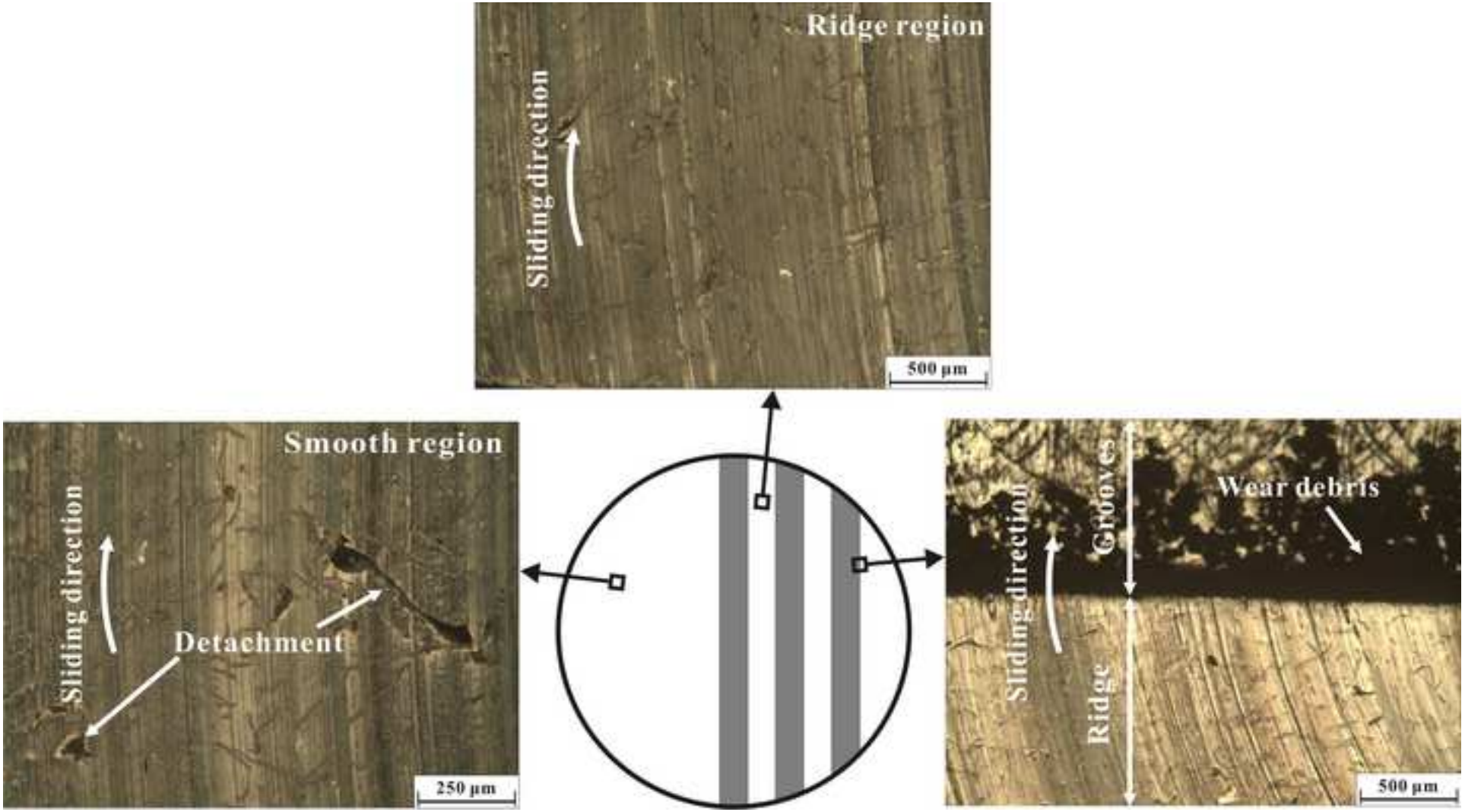

Fig. 11

Click here to download high resolution image

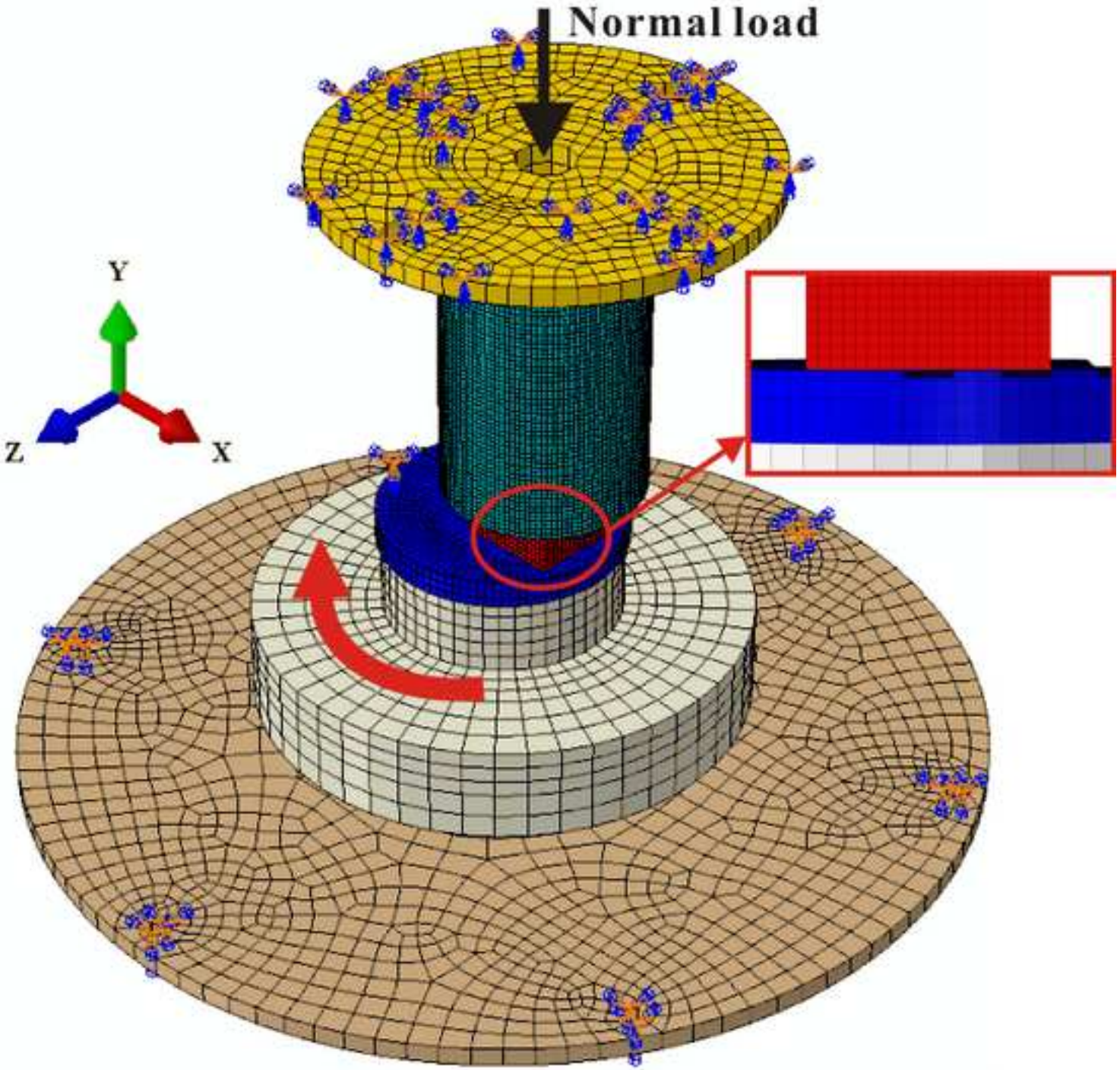

Fig. 12

Click here to download high resolution image

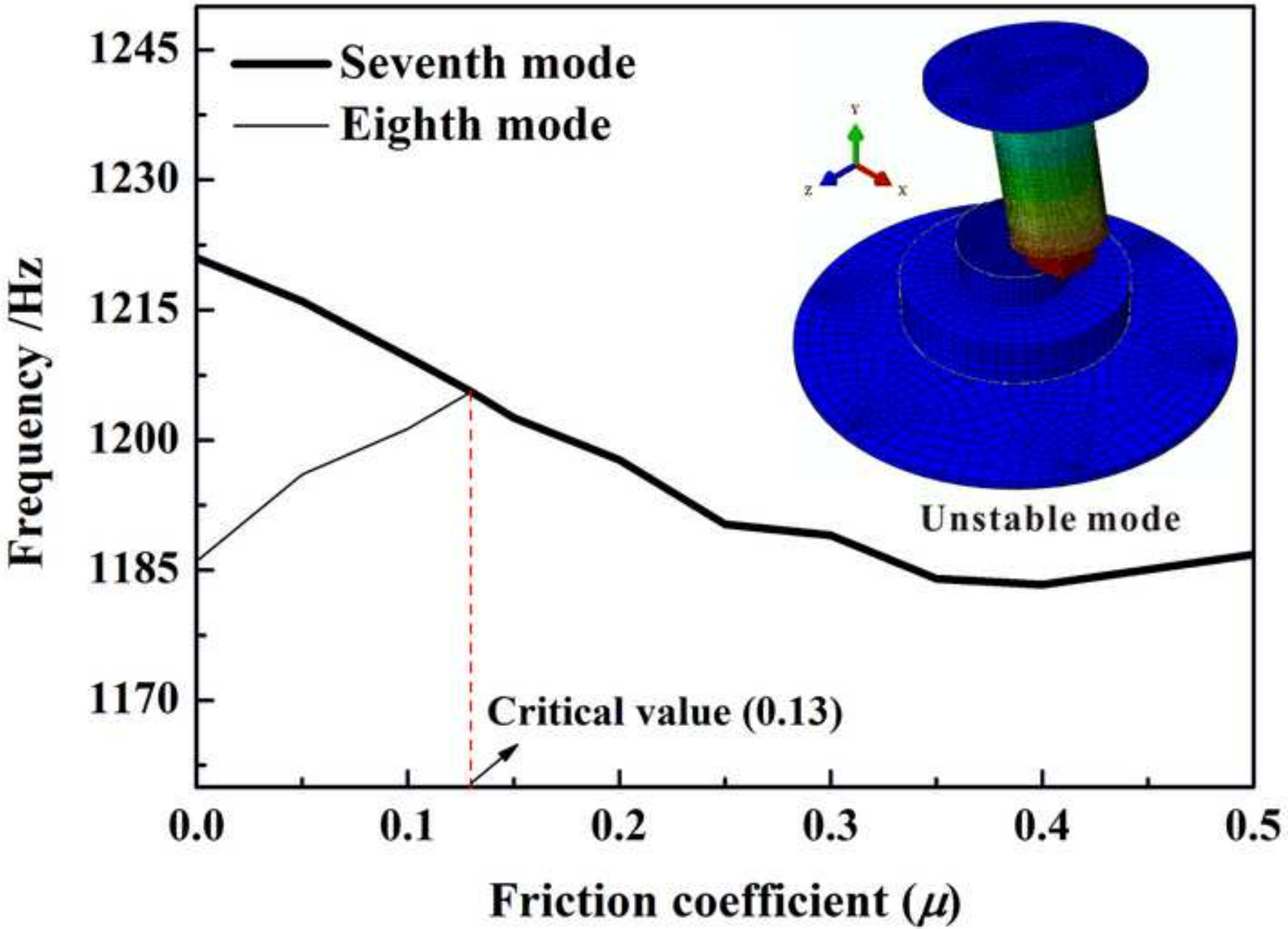

Fig. 13

Click here to download high resolution image

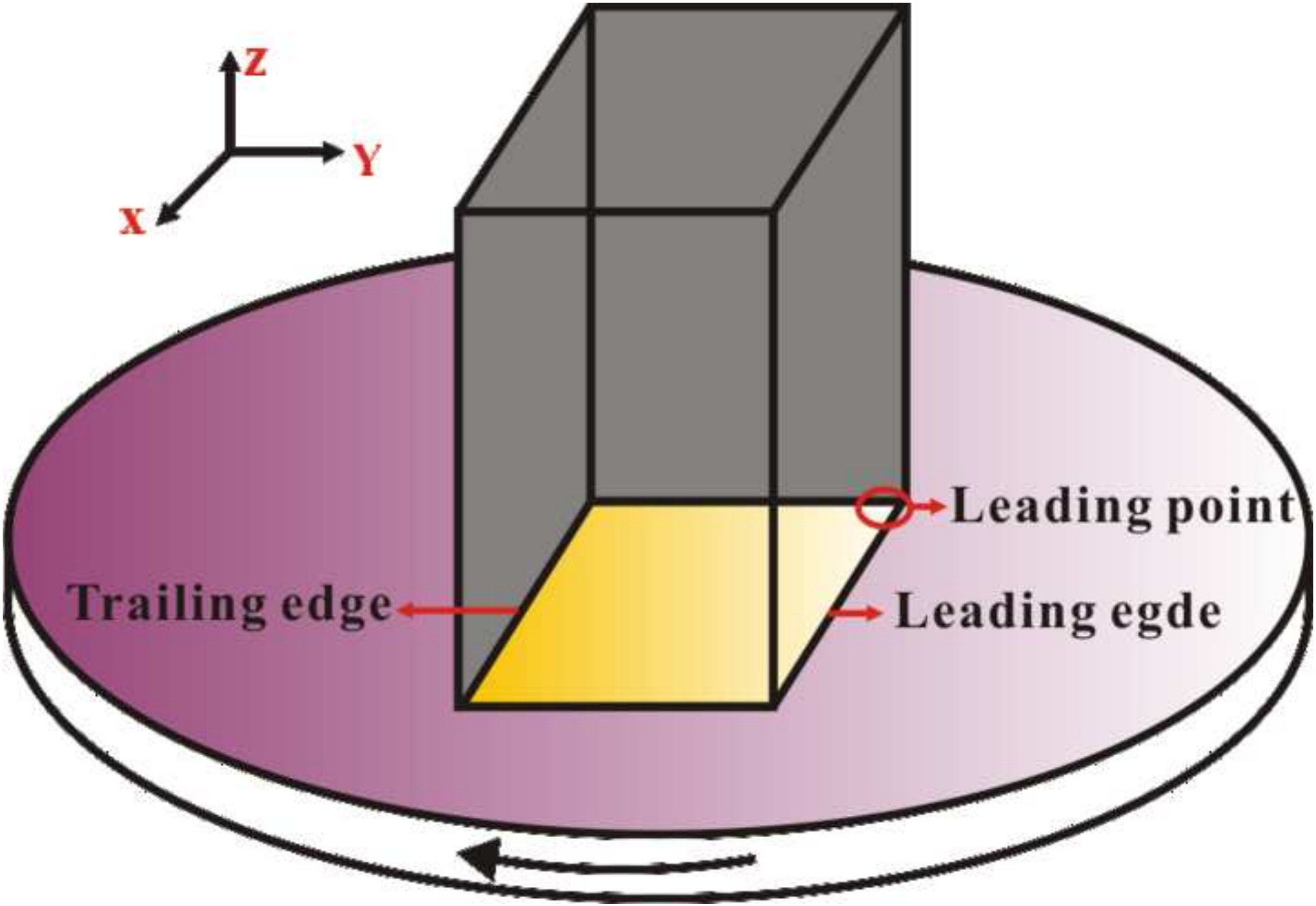

Fig. 14(a)

Click here to download high resolution image

(a)

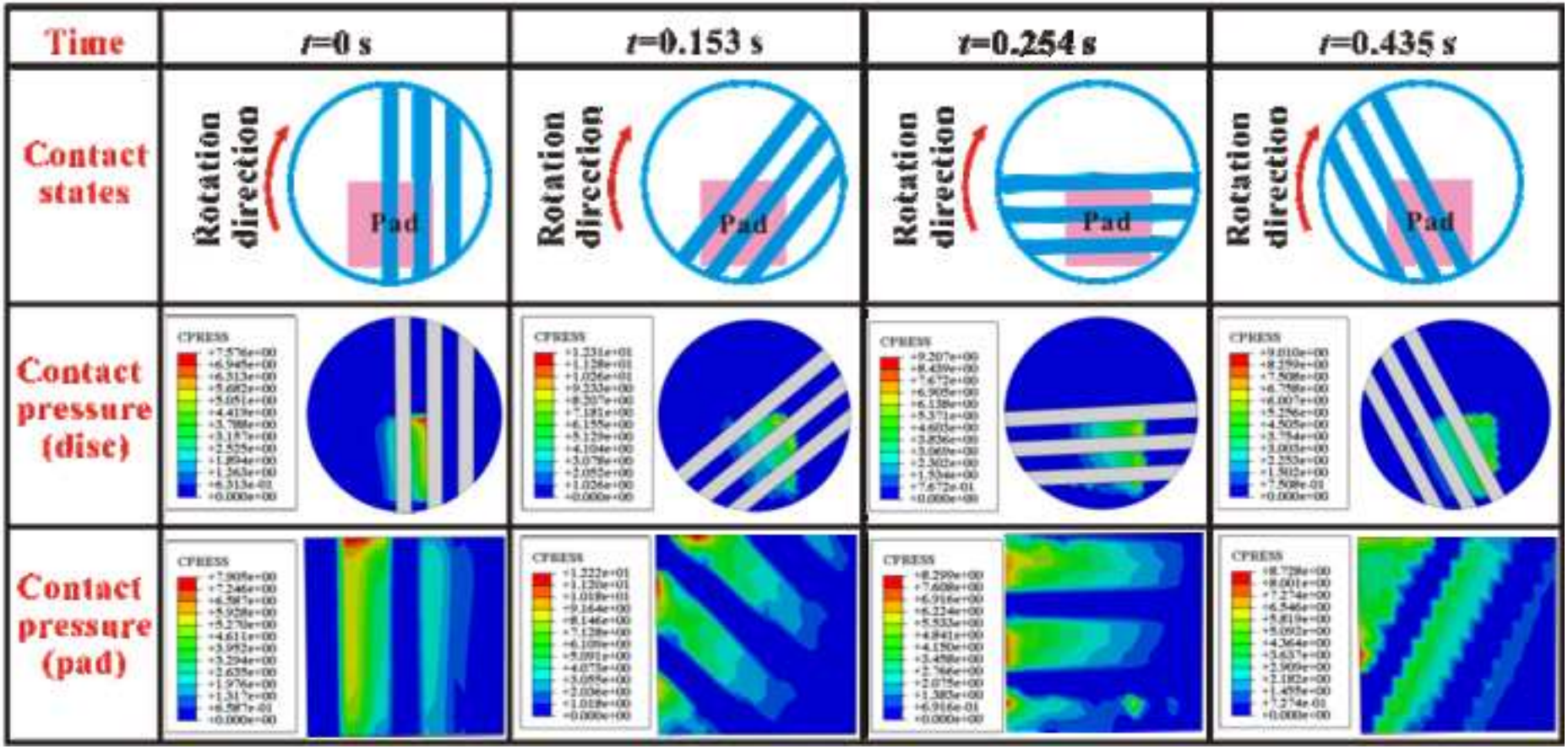

Fig. 14(b)

Click here to download high resolution image

(b)

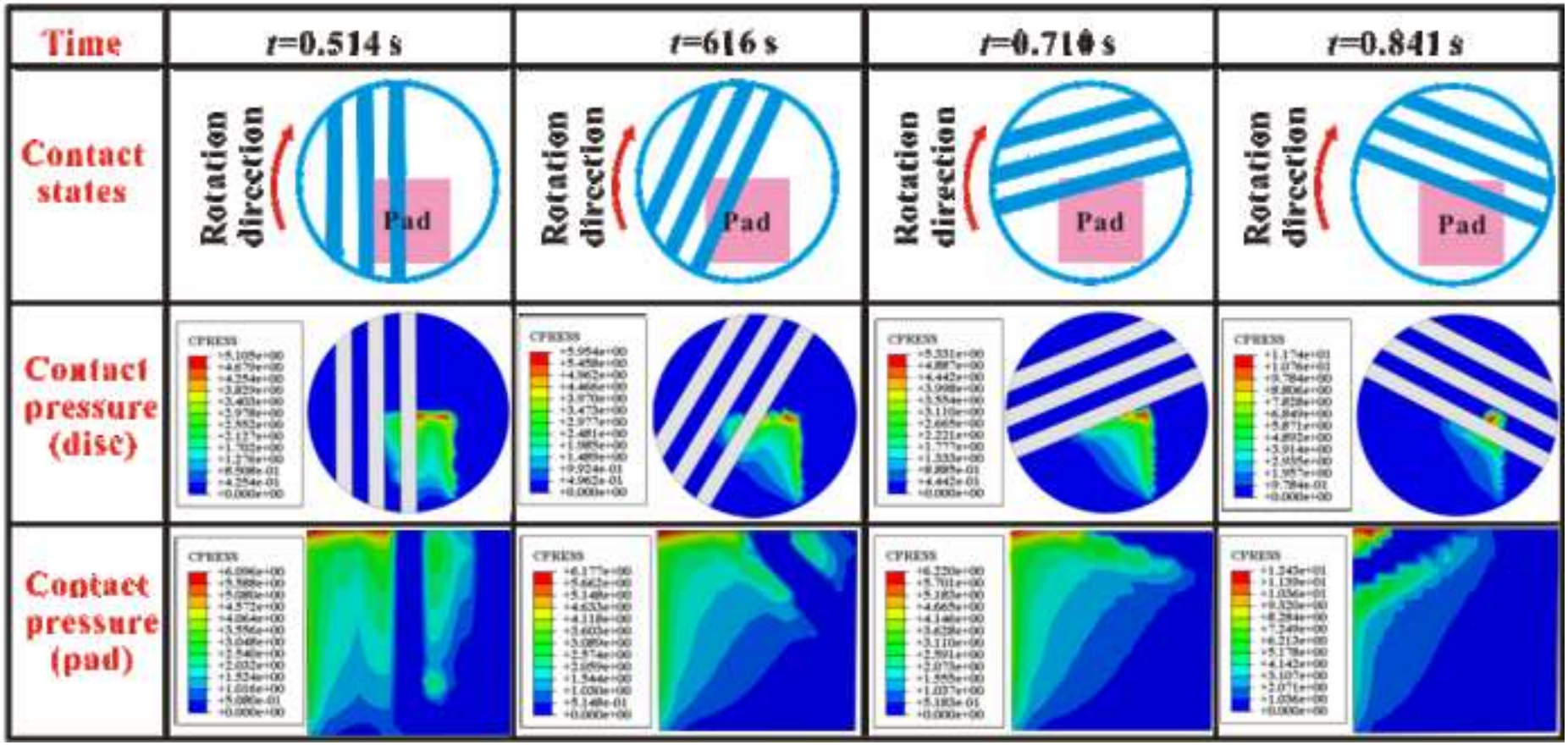

Fig. 15

Click here to download high resolution image

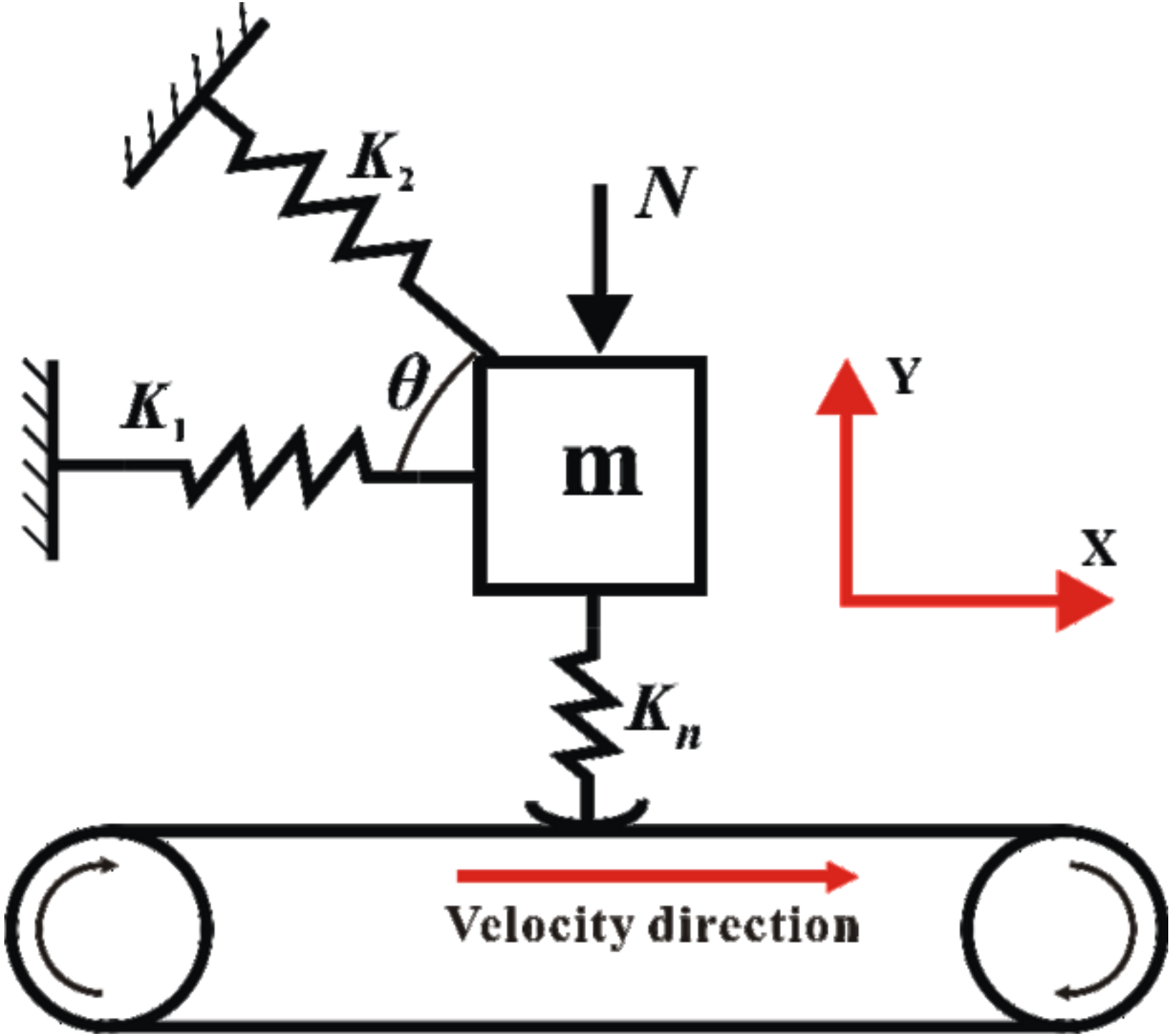

Fig. 16(a)

Click here to download high resolution image

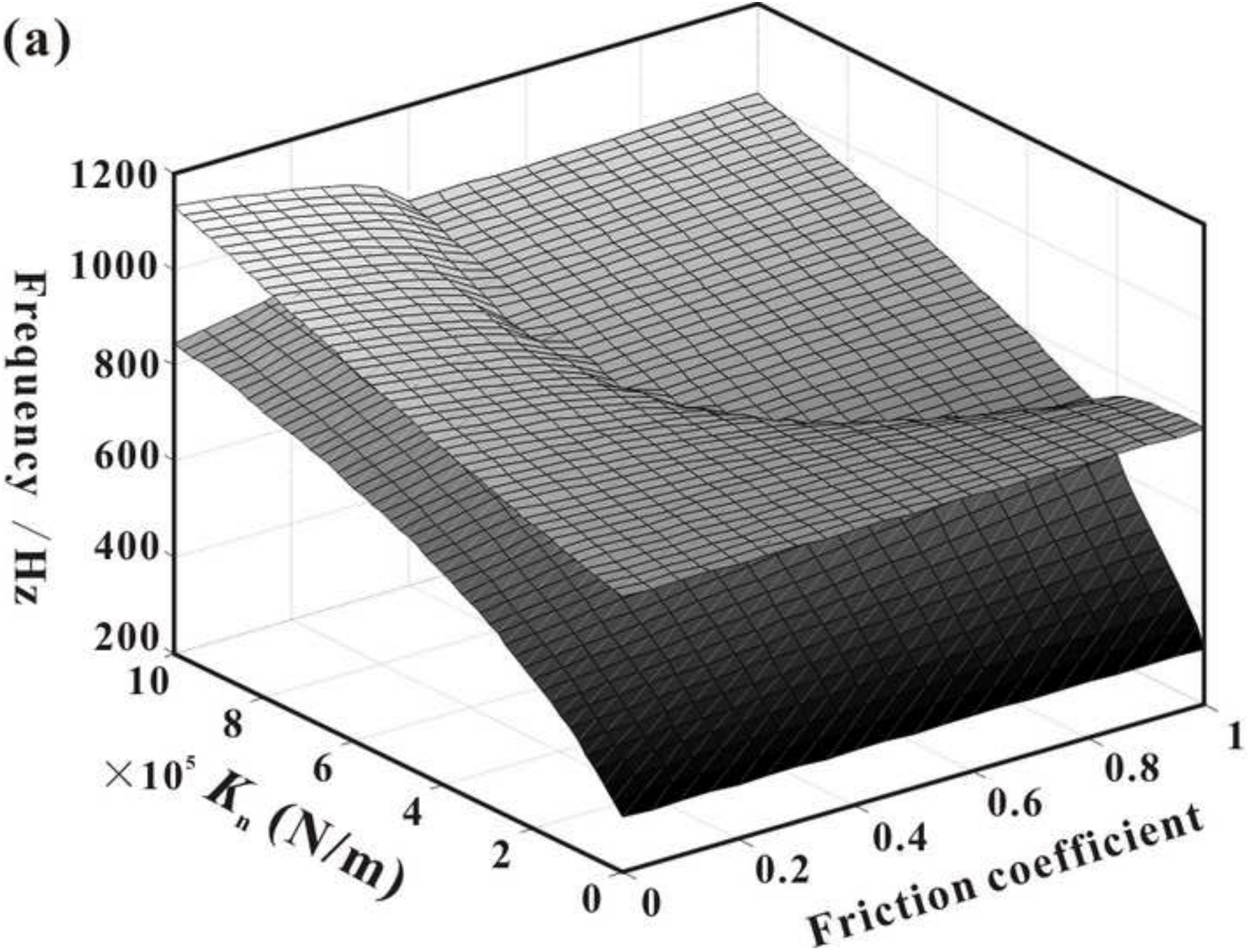

Fig. 16(b)
Click here to download high resolution image

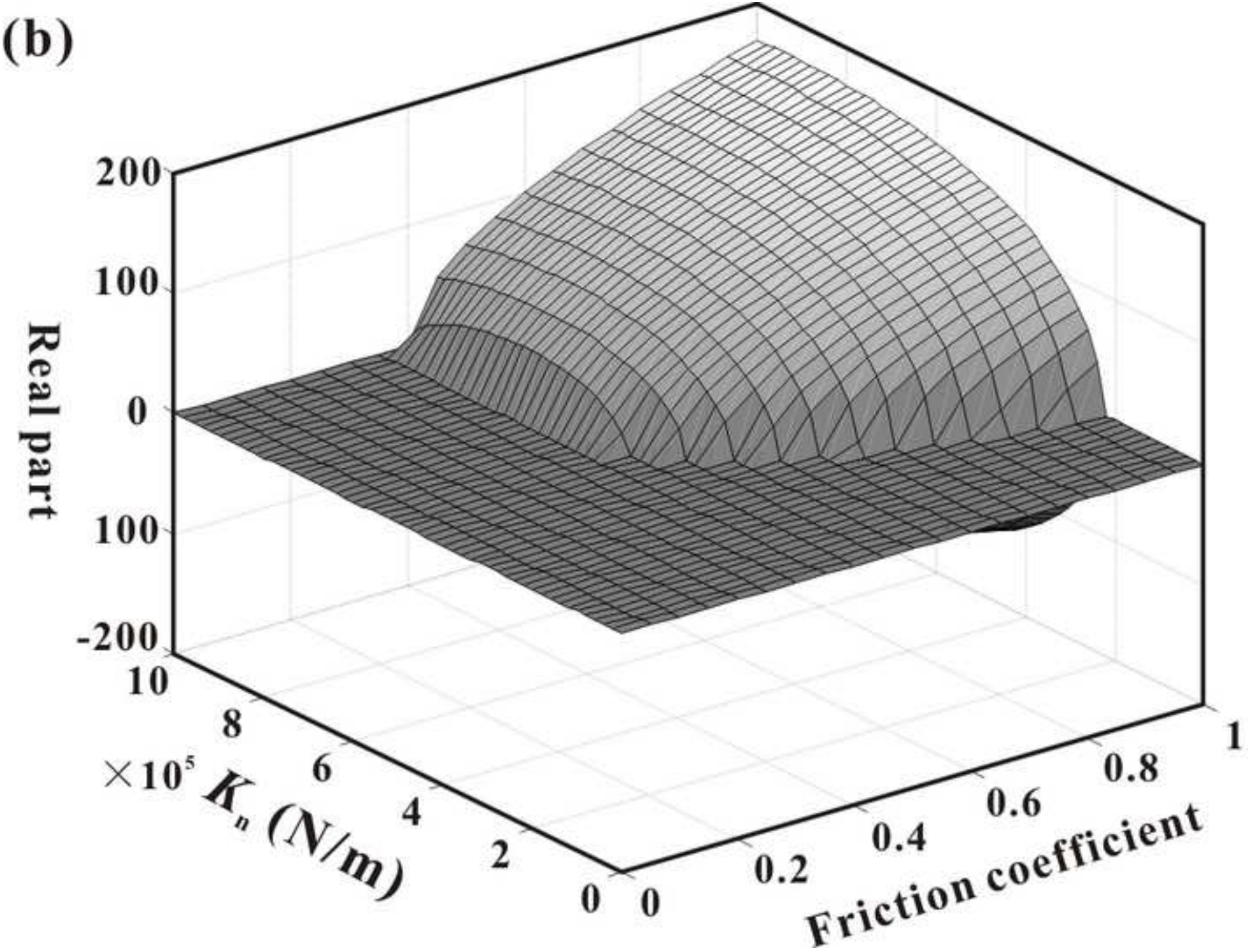

Fig. 17

Click here to download high resolution image